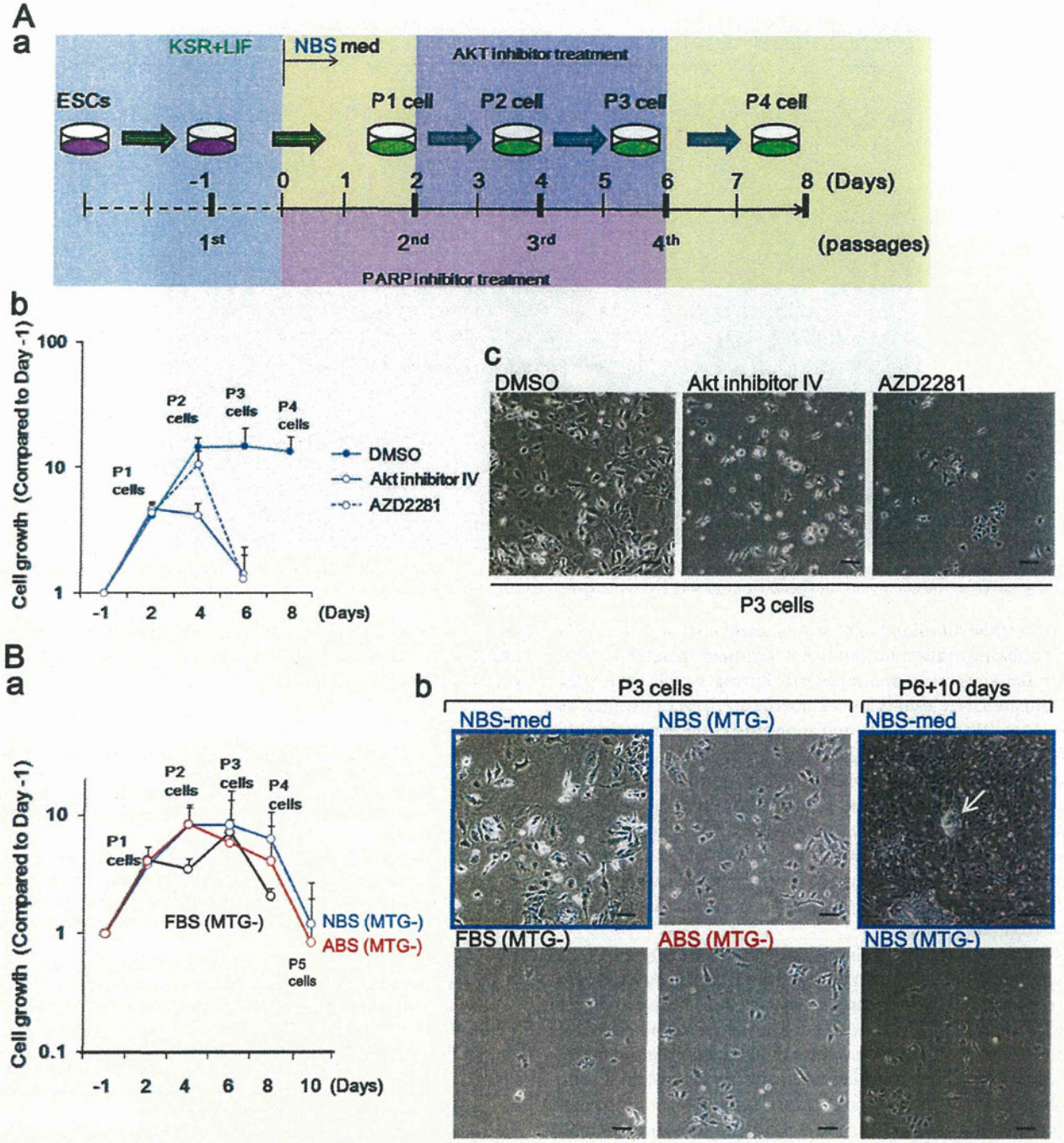

FIGURE 8. **Sufficient barrier response protects differentiating ESCs from senescence, preventing the development of cancerous stem cells.** *A*, protection of differentiating ESCs from senescence by treatment with anti-cancer drugs is shown. The experimental scheme is shown (*a*). Akt inhibitor IV and PARP inhibitor AZD2281 led to the reduction of surviving cells (*b*) and senescent cells (*c*). *B*, prevention of cancerous stem cell development in the presence of ROS is shown. Development of cancerous stem cells under NBS-med was inhibited in the absence of monothioglycerol (*MTG*) as shown in the lower cell survival (a, compared with Fig. 6*A*), inhibition of senescence (*b*, *P3 cells*), and no piled-up sphere development (*b*, *P6 + 10 days*). The *arrow* indicates the sphere development in control conditions. *Scale bars*, 50 μm.

DISCUSSION

Our results illustrated that ESCs differentiating under aberrant conditions, such as cultivation in NBS-med, are subject to carcinogenic stress, resulting in genomic instability, mutation in the *p53* locus, and the appearance of cancerous stem cells (Fig. 9). Although senescing MEFs subjected to carcinogenic stress develop immortality without accompanying stemness and tumorigenicity (10), similar stresses in differentiating ESCs are associated with the development of malignancy. Thus, unlike differentiated cells, ESCs differentiating under environmental aberrancy suffer potentially from a risk of developing into cancerous stem cells upon spontaneous exposure to carcinogenic stress.

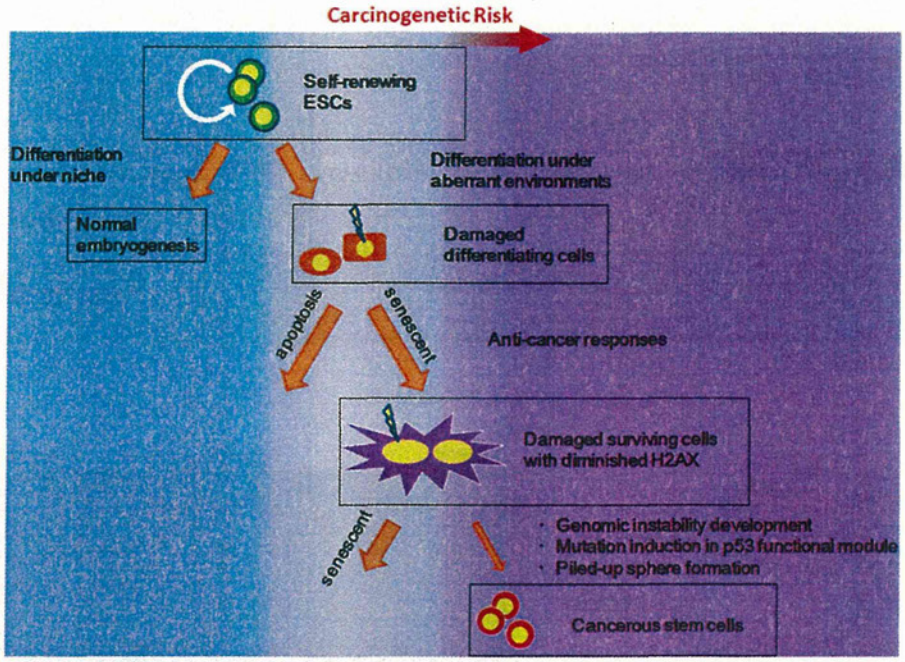

FIGURE 9. **Model.** In the process of ESC differentiation, cells subjected to environmental aberrancies are subjected to carcinogenic stress, resulting in the emergence of cancerous stem cells with genomic instability and mutations in p53 or Arf-p53 pathways.

Before their development into cancerous stem cells, ESCs differentiating in aberrant serum environments emulate cells in the initial stages of carcinogenesis, during which time they accumulate DNA lesions and exhibit barrier reactions, such as the induction of senescence and apoptosis. Genomic instability and mutations are also induced during the initial stages, contributing not only to the development of immortality but also to the acquisition of aberrant stemness characteristics that include the retention of stemness marker gene expression even under differentiation conditions. Thus, cancerous stem cells can propagate without losing stemness properties even in environments in which normal stem cells cannot maintain their undifferentiated status.

The development of CSCs is critical for carcinogenesis. In a manner analogous to the transformation of ESCs into cancerous stem cells, differentiating somatic stem cells can also be transformed into CSCs *in vivo* due to aberrant niche environments. This is supported by several documented observations: 1) age is a risk factor for defective niche function (23), 2) hematopoietic stem cells spontaneously accumulate endogenous DNA damage with age (49), and 3) disruption of the hematopoietic niche induces differentiation disorders in progenitor cells and secondary oncogenesis (22). In addition, humoral factors could be involved in the balance between progression and prevention of carcinogenic transformation; differentiating ESCs under NBS-med override the anti-cancer barrier and result in the development of cancerous stem cells, whereas those under FBS- and ABS-med are blocked. Importantly, this indicates that some conditions effectively induce anti-cancer barriers, as observed in FBS- and ABS-med, although this balance can also be altered by exogenous DNA damage. Thus, our results illustrate that normal stem cells can transform into CSCs during differentiation in aberrant environments and suggest that the development of CSCs is prevented by effective induction of anti-cancer barrier responses, pointing to a potential target for cancer prevention.

REFERENCES

1. Wicha, M. S., Liu, S., and Dontu, G. (2006) Cancer stem cells. An old idea, a paradigm shift. *Cancer Res.* **66,** 1883–1890
2. Werbowetski-Ogilvie, T. E., and Bhatia, M. (2008) Pluripotent human stem cell lines. What we can learn about cancer initiation. *Trends Mol. Med.* **14,** 323–332
3. Chiba, T., Zheng, Y. W., Kita, K., Yokosuka, O., Saisho, H., Onodera, M., Miyoshi, H., Nakano, M., Zen, Y., Nakanuma, Y., Nakauchi, H., Iwama, A., and Taniguchi, H. (2007) Enhanced self-renewal capability in hepatic stem/progenitor cells drives cancer initiation. *Gastroenterology* **133,** 937–950
4. Liu, Y., Clem, B., Zuba-Surma, E. K., El-Naggar, S., Telang, S., Jenson, A. B., Wang, Y., Shao, H., Ratajczak, M. Z., Chesney, J., and Dean, D. C. (2009) Mouse fibroblasts lacking RB1 function form spheres and undergo reprogramming to a cancer stem cell phenotype. *Cell Stem Cell* **4,** 336–347
5. Bartkova, J., Horejsí, Z., Koed, K., Krämer, A., Tort, F., Zieger, K., Guldberg, P., Sehested, M., Nesland, J. M., Lukas, C., Ørntoft, T., Lukas, J., and Bartek, J. (2005) DNA damage response as a candidate anti-cancer barrier in early human tumorigenesis. *Nature* **434,** 864–870
6. Gorgoulis, V. G., Vassiliou, L. V., Karakaidos, P., Zacharatos, P., Kotsinas, A., Liloglou, T., Venere, M., Ditullio, R. A., Jr., Kastrinakis, N. G., Levy, B., Kletsas, D., Yoneta, A., Herlyn, M., Kittas, C., and Halazonetis, T. D. (2005) Activation of the DNA damage checkpoint and genomic instability in human precancerous lesions. *Nature* **434,** 907–913
7. Bartkova, J., Rezaei, N., Liontos, M., Karakaidos, P., Kletsas, D., Issaeva, N., Vassiliou, L. V., Kolettas, E., Niforou, K., Zoumpourlis, V. C., Takaoka, M., Nakagawa, H., Tort, F., Fugger, K., Johansson, F., Sehested, M., Andersen, C. L., Dyrskjot, L., Ørntoft, T., Lukas, J., Kittas, C., Helleday, T., Halazonetis, T. D., Bartek, J., and Gorgoulis, V. G. (2006) Oncogene-induced senescence is part of the tumorigenesis barrier imposed by DNA damage checkpoints. *Nature* **444,** 633–637
8. Ichijima, Y., Yoshioka, K., Yoshioka, Y., Shinohe, K., Fujimori, H., Unno, J., Takagi, M., Goto, H., Inagaki, M., Mizutani, S., and Teraoka, H. (2010) DNA lesions induced by replication stress trigger mitotic aberration and

tetraploidy development. *PLoS One* **5,** e8821
9. Matheu, A., Maraver, A., Klatt, P., Flores, I., Garcia-Cao, I., Borras, C., Flores, J. M., Viña, J., Blasco, M. A., and Serrano, M. (2007) Delayed ageing through damage protection by the *Arf/p53* pathway. *Nature* **448,** 375–379
10. Sun, H., and Taneja, R. (2007) Analysis of transformation and tumorigenicity using mouse embryonic fibroblast cells. *Methods Mol. Biol.* **383,** 303–310
11. Yang, Y. M., and Chang, J. W. (2008) Current status and issues in cancer stem cell study. *Cancer Invest.* **26,** 741–755
12. Kim, J. H., Kim, S. H., Hahn, E. W., and Song, C. W. (1978) 5-Thio-D-glucose selectively potentiates hyperthermic killing of hypoxic tumor cells. *Science* **200,** 206–207
13. Bunting, K. D. (2002) ABC transporters as phenotypic markers and functional regulators of stem cells. *Stem Cells* **20,** 11–20
14. Seaberg, R. M., and van der Kooy, D. (2003) Stem and progenitor cells. The premature desertion of rigorous definitions. *Trends Neurosci.* **26,** 125–131
15. Leahy, A., Xiong, J. W., Kuhnert, F., and Stuhlmann, H. (1999) Use of developmental marker genes to define temporal and spatial patterns of differentiation during embryoid body formation. *J. Exp. Zool.* **284,** 67–81
16. Kondoh, H., Lleonart, M. E., Gil, J., Wang, J., Degan, P., Peters, G., Martinez, D., Carnero, A., and Beach, D. (2005) Glycolytic enzymes can modulate cellular life span. *Cancer Res.* **65,** 177–185
17. Dontu, G., El-Ashry, D., and Wicha, M. S. (2004) Breast cancer, stem/progenitor cells, and the estrogen receptor. *Trends Endocrinol. Metab.* **15,** 193–197
18. Jones, D. L., and Wagers, A. J. (2008) No place like home. Anatomy and function of the stem cell niche. *Nat. Rev. Mol. Cell Biol.* **9,** 11–21
19. Knoepfler, P. S. (2009) Deconstructing stem cell tumorigenicity. A roadmap to safe regenerative medicine. *Stem Cells* **27,** 1050–1056
20. Morange, M. (2006) What history tells us VII. Twenty-five years ago. The production of mouse embryonic stem cells. *J. Biosci.* **31,** 537–541
21. Wylie, C. (1999) Germ cells. *Cell* **96,** 165–174
22. Raaijmakers, M. H., Mukherjee, S., Guo, S., Zhang, S., Kobayashi, T., Schoonmaker, J. A., Ebert, B. L., Al-Shahrour, F., Hasserjian, R. P., Scadden, E. O., Aung, Z., Matza, M., Merkenschlager, M., Lin, C., Rommens, J. M., and Scadden, D. T. (2010) Bone progenitor dysfunction induces myelodysplasia and secondary leukemia. *Nature* **464,** 852–857
23. Smith, J. A., and Daniel, R. (2012) Stem cells and aging: a chicken-or-the-egg issue? *Aging Dis.* **3,** 260–268
24. Fujimori, H., Asahina, K., Shimizu-Saito, K., Ikeda, R., Tanaka, Y., Teramoto, K., Morita, I., and Teraoka, H. (2008) Vascular endothelial growth factor promotes proliferation and function of hepatocyte-like cells in embryoid bodies formed from mouse embryonic stem cells. *J. Hepatol.* **48,** 962–973
25. Marusyk, A., Wheeler, L. J., Mathews, C. K., and DeGregori, J. (2007) p53 mediates senescence-like arrest induced by chronic replication stress. *Mol. Cell. Biol.* **27,** 5336–5351
26. Fernandes, K. J., McKenzie, I. A., Mill, P., Smith, K. M., Akhavan, M., Barnabé-Heider, F., Biernaskie, J., Junek, A., Kobayashi, N. R., Toma, J. G., Kaplan, D. R., Labosky, P. A., Rafuse, V., Hui, C. C., and Miller, F. D. (2004) A dermal niche for multipotent adult skin-derived precursor cells. *Nat. Cell Biol.* **6,** 1082–1093
27. Lee, B. Y., Han, J. A., Im, J. S., Morrone, A., Johung, K., Goodwin, E. C., Kleijer, W. J., DiMaio, D., and Hwang, E. S. (2006) Senescence-associated β-galactosidase is lysosomal β-galactosidase. *Aging Cell* **5,** 187–195
28. Masaki, H., Nishida, T., Kitajima, S., Asahina, K., and Teraoka, H. (2007) Developmental pluripotency-associated 4 (DPPA4) localized in active chromatin inhibits mouse embryonic stem cell differentiation into a primitive ectoderm lineage. *J. Biol. Chem.* **282,** 33034–33042
29. Nitou, M., Sugiyama, Y., Ishikawa, K., and Shiojiri, N. (2002) Purification of fetal mouse hepatoblasts by magnetic beads coated with monoclonal anti-e-cadherin antibodies and their *in vitro* culture. *Exp. Cell Res.* **279,** 330–343
30. Lengauer, C., Kinzler, K. W., and Vogelstein, B. (1998) Genetic instabilities in human cancers. *Nature* **396,** 643–649
31. Sherr, C. J., and McCormick, F. (2002) The RB and p53 pathways in cancer. *Cancer Cell* **2,** 103–112
32. Zhang, P., Andrianakos, R., Yang, Y., Liu, C., and Lu, W. (2010) Kruppel-like factor 4 (Klf4) prevents embryonic stem (ES) cell differentiation by regulating Nanog gene expression. *J. Biol. Chem.* **285,** 9180–9189
33. Jain, A. K., Allton, K., Iacovino, M., Mahen, E., Milczarek, R. J., Zwaka, T. P., Kyba, M., and Barton, M. C. (2012) p53 regulates cell cycle and microRNAs to promote differentiation of human embryonic stem cells. *PLoS Biol.* **10,** e1001268
34. Ferrandina, G., Petrillo, M., Bonanno, G., and Scambia, G. (2009) Targeting CD133 antigen in cancer. *Expert Opin. Ther. Targets* **13,** 823–837
35. Takahashi, K., and Yamanaka, S. (2006) Induction of pluripotent stem cells from mouse embryonic and adult fibroblast cultures by defined factors. *Cell* **126,** 663–676
36. Spierings, D. C., de Vries, E. G., Vellenga, E., and de Jong, S. (2003) The attractive Achilles heel of germ cell tumors. An inherent sensitivity to apoptosis-inducing stimuli. *J. Pathol.* **200,** 137–148
37. Oh, S. K., and Choo, A. B. (2006) Human embryonic stem cells. Technological challenges toward therapy. *Clin. Exp. Pharmacol. Physiol.* **33,** 489–495
38. Atsumi, Y., Fujimori, H., Fukuda, H., Inase, A., Shinohe, K., Yoshioka, Y., Shikanai, M., Ichijima, Y., Unno, J., Mizutani, S., Tsuchiya, N., Hippo, Y., Nakagama, H., Masutani, M., Teraoka, H., and Yoshioka, K. (2011) Onset of quiescence following p53-mediated down-regulation of H2AX in normal cells. *PLoS One* **6,** e23432
39. Yoshioka, K., Atsumi, Y., Fukuda, H., Masutani, M., and Teraoka, H. (2012) The quiescent cellular state is *Arf/p53*-dependent and associated with H2AX down-regulation and genome stability. *Int. J. Mol. Sci.* **13,** 6492–6506
40. Celeste, A., Difilippantonio, S., Difilippantonio, M. J., Fernandez-Capetillo, O., Pilch, D. R., Sedelnikova, O. A., Eckhaus, M., Ried, T., Bonner, W. M., and Nussenzweig, A. (2003) H2AX haploinsufficiency modifies genomic stability and tumor susceptibility. *Cell* **114,** 371–383
41. Woo, R. A., and Poon, R. Y. (2004) Activated oncogenes promote and cooperate with chromosomal instability for neoplastic transformation. *Genes Dev.* **18,** 1317–1330
42. Deckbar, D., Birraux, J., Krempler, A., Tchouandong, L., Beucher, A., Walker, S., Stiff, T., Jeggo, P., and Löbrich, M. (2007) Chromosome breakage after G_2 checkpoint release. *J. Cell Biol.* **176,** 749–755
43. Oh, S. J., Erb, H. H., Hobisch, A., Santer, F. R., and Culig, Z. (2012) Sorafenib decreases proliferation and induces apoptosis of prostate cancer cells by inhibition of the androgen receptor and Akt signaling pathways. *Endocr. Relat. Cancer* **19,** 305–319
44. Mitsiades, C. S., Mitsiades, N., and Koutsilieris, M. (2004) The Akt pathway. Molecular targets for anti-cancer drug development. *Curr. Cancer Drug Targets* **4,** 235–256
45. Fong, P. C., Boss, D. S., Yap, T. A., Tutt, A., Wu, P., Mergui-Roelvink, M., Mortimer, P., Swaisland, H., Lau, A., O'Connor, M. J., Ashworth, A., Carmichael, J., Kaye, S. B., Schellens, J. H., and de Bono, J. S. (2009) Inhibition of poly(ADP-ribose) polymerase in tumors from BRCA mutation carriers. *N. Engl. J. Med.* **361,** 123–134
46. Parrinello, S., Samper, E., Krtolica, A., Goldstein, J., Melov, S., and Campisi, J. (2003) Oxygen sensitivity severely limits the replicative lifespan of murine fibroblasts. *Nat. Cell Biol.* **5,** 741–747
47. Wiles, M. V., and Keller, G. (1991) Multiple hematopoietic lineages develop from embryonic stem (ES) cells in culture. *Development* **111,** 259–267
48. Guachalla, L. M., and Rudolph, K. L. (2010) ROS induced DNA damage and checkpoint responses. Influences on aging? *Cell Cycle* **9,** 4058–4060
49. Rossi, D. J., Bryder, D., Seita, J., Nussenzweig, A., Hoeijmakers, J., and Weissman, I. L. (2007) Deficiencies in DNA damage repair limit the function of hematopoietic stem cells with age. *Nature* **447,** 725–729

Yoshimi et al. BMC Cancer 2012, 12:448
http://www.biomedcentral.com/1471-2407/12/448

BMC Cancer

RESEARCH ARTICLE Open Access

Use of a chemically induced-colon carcinogenesis-prone *Apc*-mutant rat in a chemotherapeutic bioassay

Kazuto Yoshimi[1], Takao Hashimoto[2], Yusuke Niwa[2], Kazuya Hata[2], Tadao Serikawa[1], Takuji Tanaka[3] and Takashi Kuramoto[1*]

Abstract

Background: Chemotherapeutic bioassay for colorectal cancer (CRC) with a rat model bearing chemically-induced CRCs plays an important role in the development of new anti-tumor drugs and regimens. Although several protocols to induce CRCs have been developed, the incidence and number of CRCs are not much enough for the efficient bioassay. Recently, we established the very efficient system to induce CRCs with a chemically induced-colon carcinogenesis-prone *Apc*-mutant rat, Kyoto Apc Delta (KAD) rat. Here, we applied the KAD rat to the chemotherapeutic bioassay for CRC and showed the utility of the KAD rat.

Methods: The KAD rat has been developed by the ENU mutagenesis and carries a homozygous nonsense mutation in the *Apc* gene (S2523X). Male KAD rats were given a single subcutaneous injection of AOM (20 mg/kg body weight) at 5 weeks of age. Starting at 1 week after the AOM injection, they were given 2% DSS in drinking water for 7 days. Tumor-bearing KAD rats were divided into experimental and control groups on the basis of the number of tumors observed by endoscopy at week 8. The 5-fluorouracil (5-FU) was administrated intravenously a dose of 50 or 75 mg/kg weekly at week 9, 10, and 11. After one-week interval, the 5-FU was given again at week 13, 14, and 15. At week 16, animals were sacrificed and tumor number and volume were measured macroscopically and microscopically.

Results: In total 48 tumors were observed in 27 KAD rats with a 100% incidence at week 8. The maximum tolerated dose for the KAD rat was 50 mg/kg of 5-FU. Macroscopically, the number or volume of tumors in the 5-FU treated rats was not significantly different from the control. Microscopically, the number of adenocarcinoma in the 5-FU treated rats was not significantly different ($p < 0.02$) from that of the control. However, the volume of adenocarcinomas was significantly lower than in the control. Anticancer effect of the 5-FU could be obtained only after the 16 weeks of experimental period.

Conclusion: The use of the AOM/DSS-treated tumor-bearing KAD rats could shorten the experimental period and reduce the number of animals examined in the chemotherapeutic bioassay. The efficient bioassay with the AOM/DSS-treated tumor-bearing KAD rats would promote the development of new anti-tumor drugs and regimens.

Keywords: Adenomatous polyposis coli, Colorectal cancer, Endoscopy, Rat, Chemotherapy, 5-fluorouracil

* Correspondence: tkuramot@anim.med.kyoto-u.ac.jp
[1]Institute of Laboratory Animals, Graduate School of Medicine, Kyoto University, Yoshidakonoe-cho, Sakyo-ku, Kyoto 606-8501, Japan
Full list of author information is available at the end of the article

Background

Chemotherapeutic bioassays for colorectal cancer (CRC) play an important role in the development of new anti-tumor drugs and regimens. These bioassays involve the use of colon carcinogenesis models which mainly consist of animal xenografts, an adenomatous polyposis coli (*Apc*)-mutant mouse model and a chemically-induced CRC model [1-3].

The xenograft model utilizes cultured or primary CRC cells that are implanted under the skin of immune-deficient mice and rats. The size and volume of tumors can be estimated easily and temporally by measuring their dimensions. However, these animals have defects in the immune system that suppresses tumor growth. The subcutaneous microenvironment around the transplanted tumors differs from the colon environment in which the original CRC of the cell lines arose. Therefore, this approach appears to ignore the contribution of the tumor microenvironment and does not exactly mimic tumor development in man [4,5].

Apc-mutant mouse models, such as the Min mouse model, spontaneously develop a considerable number of intestinal tumors and have been widely used as a relevant model for evaluating human chemopreventative therapies. However, tumors in the colon are developed at a much lower frequency than in the small intestine. Even if tumors do develop in the colon, almost all of them are low grade adenomas [6].

The chemically-induced CRC model is superior to these models in that the characteristics of the induced tumor are very similar to those of human CRC. Tumors only develop in the colon through multi-step carcinogenesis which mimics the entire process of tumor growth in man. In this model, tumor morphology and mutation spectrum are also similar to those in human CRC [6]. Moreover, methods of inducing colon tumors are well-established, so that we can be certain of obtaining the number of tumors expected, which is ideal for the evaluation of potential chemotherapeutic drugs [2,7].

Although many carcinogens induce colon tumors in rats, azoxymethane (AOM) administered subcutaneously has been most widely used [2,6,8]. However, the incidence of colon tumors induced by two or three subcutaneous injections of AOM is not high, and it takes 7–9 months to induce sufficient tumors to evaluate the chemotherapeutic efficacy of potential anti-cancer drugs [9]. Such limitations have been significantly improved by using dextran sodium sulfate (DSS) as an inflammatory agent. When 2% DSS is administered in drinking water to the AOM-treated rats for one week, starting one week after administration, a number of colon tumors develop within a short time period (this is known as the TANAKA method) [10].

Recently we developed a novel *Apc* mutant rat strain, called the Kyoto Apc Delta (KAD) rat (strain name: F344-*Apc*^{m1kyo}) from our ENU-mutagenesis program. The KAD rat carries a homozygous nonsense mutation in the *Apc* gene (S2523X). Thus, the KAD rat lacks 321-amino acids in the C-terminal of APC, but it remains viable at almost 2 years and shows no spontaneous colorectal tumors. Moreover, by applying the TANAKA method to KAD rats, we obtained a much higher incidence, multiplicity and malignancy of colon tumors in KAD rats than colon tumors in F344 wild rats. We were able to induce these tumors within 15 weeks of the experimental period. In addition, we were able to carry out endoscopic observation, by which colon tumors could be detected from Week 8 [11].

In the present study, in order to establish an efficient chemotherapeutic bioassay with KAD rats, we induced colon tumors by means of treatment with AOM and DSS, and then administered a typical anti-tumor drug, namely 5-fluorouracil (5-FU) to the tumor-bearing rats.

Methods

Chemicals

5-FU was purchased from Kyowa Hakko Kogyo, Co., Ltd. (Tokyo, Japan). AOM was purchased from Sigma-Aldrich Chemical Co. (St. Louis, MO, USA). These drugs were diluted in saline just before administration. DSS (MW 36,000–50,000) was purchased from ICN Biochemicals, Inc. (Aurora, OH, USA). DSS was dissolved in distilled water at 2% (w/v) every day before treatment.

Rats

Specific pathogen free male KAD rats were purchased from Japan SLC, Inc. (Hamamatsu, Japan) and provided by the National Bio Resource Project for the Rat (http://www.anim.med.kyoto-u.ac.jp/nbr) at 4 weeks of age. The rats were acclimatized for a week before the experiment and were maintained under conditions of 50 ± 10% humidity, 12 h-12 h light cycle and 24 ± 2 °C temperature. They were fed a standard pellet diet (F-2, Funabashi Farm, Funabashi, Japan) and tap water *ad libitum*.

Induction of colon tumor

Chemically induced-colon carcinogenesis was carried out as described in our previous study [11]. Briefly, male KAD rats (n = 32) were given a single subcutaneous injection of AOM (20 mg/kg body weight) at 5 weeks of age. Starting at 1 week after the AOM injection, they were given 2% DSS in drinking water for 7 days (Figure 1). Five rats were used to find correlation of the number of polypoid lesions with the volume of tumors at Week 8. All experimental procedures were approved by the Animal Research Committee of Kyoto University

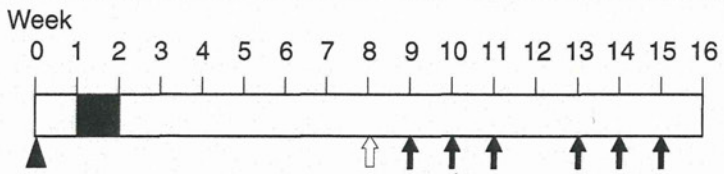

Figure 1 Experimental schedule. KAD rats at 5 weeks of age were given a subcutaneous injection of AOM at 20 mg/kg body weight (arrow head). One week after the AOM injection they were given 2% DSS (MW 36,000–50,000) in their drinking water for one week (black box). Endoscopic observation was carried out at week 8 (open arrow). 5-FU was administrated intravenously at weeks 9, 10, 11, 13, 14 and 15 (arrows). All animals were sacrificed at week 16.

and were performed according to the Regulation on Animal Experimentation at Kyoto University.

Endoscopic observation

Observation was performed at week 8 with an endoscope (BF TYPE 3C40: Olympus, Tokyo, Japan) to determine the presence of colon tumors (Figure 1). KAD rats were anesthetized by administration of 2% isoflurane (Forane: Abbott Japan, Tokyo, Japan) vapor through a nose cone. The colon was flushed using an enema of tap water to remove feces. The endoscope was inserted into the colon, and endoscopic images were acquired within the distal colon and rectum. The numbers of polypoid lesions, assumed to be developing colorectal tumors, were counted.

Chemotherapeutic test

The AOM/DSS-treated rats were divided into three groups (nine rats each), among which numbers of colon tumors were not significantly different. The 5-FU was administrated to the tumor-bearing KAD rats at two different doses (50 or 75 mg/kg) by three weekly intravenous (i.v.) injections at weeks 9, 10 and 11. According to the preliminary experiment, we set a 1 week withdrawal period to decrease the occurrence of serious side effects caused by 5-FU. One week later, rats underwent additional administration of 5-FU involving three weekly i.v. injections at weeks 13, 14 and 15. At week 16 animals were sacrificed by cervical dislocation under anesthesia with isoflurane (Figure 1). Then the colorectum of the rats was resected, washed with PBS, opened longitudinally along the main axis and fixed in 10% neutral buffered formalin for at least 24 h. The number and volume of colon tumors were measured after fixation. The other organs such as small intestine, stomach, liver and kidney were observed macroscopically for any abnormalities.

Histopathological examination

After careful macroscopic inspection, tumors and whole colonic mucosa were embedded in paraffin and sectioned for histopathology after staining with hematoxylin and eosin. After tumors that developed in the colorectum were photographed, the largest and the smallest superficial diameters of adenocarcinoma that were diagnosed histopathologically were measured on the photographs. Tumor volume was calculated according to the formula $V = a \times b^2/2$, in which "a" is the largest superficial diameter and "b" is the smallest superficial diameter [12].

Immunohistochemistry

Cell proliferation and apoptosis were evaluated by determination of the percentages of PCNA- and cleaved caspase-3-positive nuclei in a total of 200 cancer cells for each sample (n = 6 from the control group and n = 8 from Group 1). Briefly, sections were incubated with anti-mouse PCNA antibody (clone PC10, 1:1000 dilution; DAKO) and cleaved caspase-3 (Asp175) antibody (1:1000 dilution; Cell Signaling Technology) overnight at 4 °C. Biotinyl antibody was used as secondary antibody and then the streptavidin-peroxidase complex (LASB^{TM} + Kit, Universal, DAKO) was applied. The antigen-antibody complex was visualized by 3,3′-diamonobenzidine tetrachloride (DAKO).

Statistical analysis

Data are expressed as the mean ± standard deviation (S.D.). Student's *t*-test was performed using the statistics package within Microsoft Excel for statistical analysis, and p values were considered significant when < 0.05.

Results

Correlation of the number of polypoid lesions with the total volume of tumors

To find the correlation of the number of polypoid lesions with the total volume of tumors, we induced colon tumors to KAD rats (n = 5) by the TANAKA method and counted tumor number under the endoscopy and the number and volume of tumors under the microscopy at week 8 (Additional file 1: Table S1). As a good correlation between them was found, it is very likely that the number of polypoid lesions found with the endoscopy at week 8 can be used to estimate the total volume of tumors (Additional file 2: Figure S1).

Effective tumor development in AOM/DSS-treated KAD rats

At week 8 when carrying out endoscopic observations for the occurrence of colon tumors in the colons of AOM/DSS-treated KAD rats, we could observe about 10 cm of the luminal surface, from the rectum to the distal colon. We found polypoid lesions around the rectum and the distal colon. Polypoid lesions which were clearly different from normal mucosa assumed to be developing colorectal tumors. All AOM/DSS-treated KAD rats developed colon tumors. In total 48 tumors were observed in 27 KAD rats with a 100% incidence and a multiplicity of 1.78 ± 0.85, ranging from 1 to 4 per rat.

Dosing condition of 5-FU

On the basis of the number of tumors, the tumor-bearing KAD rats were divided into three groups. One was the control group and the others were experimental groups, in which rats were given 5-FU at a concentration of 50 mg/kg (Group 1) or 75 mg/kg (Group 2). Each group consisted of nine rats and the total number of tumors in each group was 16. The average number of tumors per rat was not significantly different among the groups (Control: 1.78 ± 0.83, Group 1: 1.78 ± 0.83, Group 2: 1.78 ± 0.97) (Figure 2B).

The average body weight of rats in Group 1 tended to be lower than in the control group, and was significantly different from the control group at weeks 15 (300.0 ± 18.1 vs 319.4 ± 20.1; $p < 0.05$) and 16 (296.1 ± 18.9 vs 318.8 ± 18.8; $p < 0.03$). However the reduction in body weight was less than 10% as compared with the control. None of the rats in Group 1 died during the experiment. On the other hand, gain in body weight in Group 2 was constantly and significantly impaired throughout the experimental period. More than 10% of weight loss was observed at weeks 12, 15 and 16, as compared with that in the control group (Figure 3A). KAD rats in Group 2 had severe bloody stools and diarrhea and six rats (67%) in the group died during the experiment (Figure 3B). These findings indicated that the 75 mg/kg dose of 5-FU was too toxic for the tumor-bearing KAD rats, and led to the marked body weight loss and eventually to death. Thus, the 50 mg/kg dose of 5-FU was considered to be appropriate for evaluation of the antitumor activity of 5-FU, when we used the tumor-bearing KAD rats in a chemotherapeutic bioassay.

Reduction of volume but not number of adenocarcinomas in the tumor-bearing KAD rats by treatment with 5-FU

At week 16 we carried out an autopsy and macroscopic examination of the large bowels of the control group and Group 1. Macroscopically, rats in both groups developed multiple nodular, polypoid or caterpillar-like tumors mainly in the rectum and distal colon (Figure 4). The number of tumors in Group 1 was not significantly different from the control group (Table 1). The volume of tumors, which were macroscopically calculated, was 27% smaller in Group 1 than in the control group, but the difference was not significant ($p = 0.34$).

Microscopically, all tumors that developed in KAD rats were tubular adenoma or well- or moderately-differentiated tubular adenocarcinoma (Figure 5A and 5B). The multiplicity of adenoma or adenocarcinoma in Group 1 was not significantly different from that of the control group ($p = 0.53$; $p = 0.44$, respectively) (Table 1). The size of the adenomas was too small for their volumes to be calculated. However, the volume of adenocarcinomas (63.85 ± 51.06 mm^3) in Group 1 was significantly lower ($p < 0.02$) than in the control group (34.40 ± 31.26 mm^3), when the volume was calculated from the histological sections. In addition, we found significant reduction of PCNA labeling index as well as

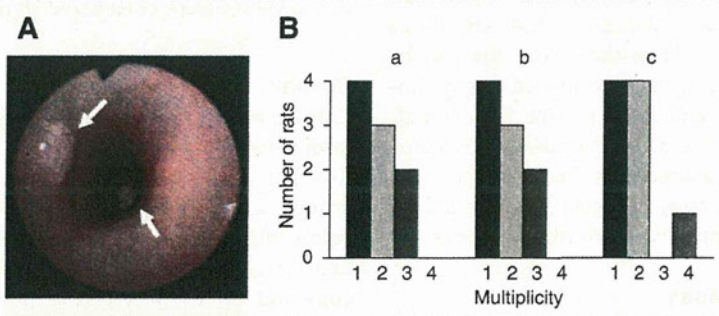

Figure 2 Grouping of AOM/DSS-treated KAD rats before 5-FU treatment. (**A**) Endoscopic view of colon tumors (arrows) in an AOM/DSS-treated KAD rat at week 8. (**B**) AOM/DSS-treated KAD rats were divided into experimental groups based on the number of tumors induced in their colons. The number of tumors induced in each animal determined by endoscopic observations varied from one to four. In total, 48 tumors were found in 27 rats. The tumor-bearing rats (nine per group) were divided into three groups (a: saline, b: 50 mg/kg 5-FU and c: 75 mg/kg 5-FU), so as not to be significantly different at the starting point of treatments.

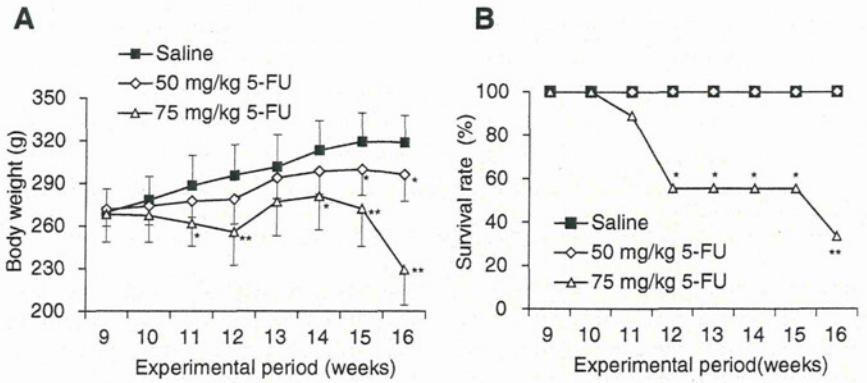

Figure 3 Toxicity of 5-FU in AOM/DSS treated KAD rats. Average body weight (**A**) and survival rate (**B**) of the control, 50 mg/kg and 75 mg/kg 5-FU treated groups. *$p < 0.05$, **$p < 0.001$.

significant elevation of cleaved caspase-3 positive rate in the adenocarcinomas in Group 1 (Figure 6). These results suggest that the 5-FU treatment suppressed cell proliferation and induced apoptosis and thereby inhibited adenocarcinoma development.

Discussion

Carcinogenic process is complex. Tumor development proceeds via a multi-step process, in which a succession of genetic changes, each conferring one or another type of growth advantage, leads to the progressive conversion of normal cells into cancer cells. Moreover, extent of cell transformation depends on the genetic predisposition and environmental factors [13]. Thus, to obtain cancerous lesions effectively, it is necessary to use a synergy effect of genetic and environmental factors. Our carcinogenic system with KAD rats employs such synergy effect of *Apc*-mutation, chemical carcinogen exposure, and tissue inflammation.

In ideal chemotherapeutic bioassay systems, the number and volume of tumors should be evaluated as the indicator of anti-tumor drug efficacy. Therefore, it is indispensable to be able to strictly set the size of the experimental and control groups, among which the number and volume of tumors should not differ significantly. To this end, we carried out endoscopic observations in the colons of AOM/DSS-treated KAD rats, and divided animals into groups on the basis of the number of colon tumors. Since the rat has a suitable body size for handling, we could easily manipulate the endoscope and correctly count the number of tumors. At week 8 we found colon tumors with a 100% incidence in AOM/DSS-treated KAD rats. The rats developed one to four tumors. On the basis of the number of tumors, we could set the experimental and control groups, because

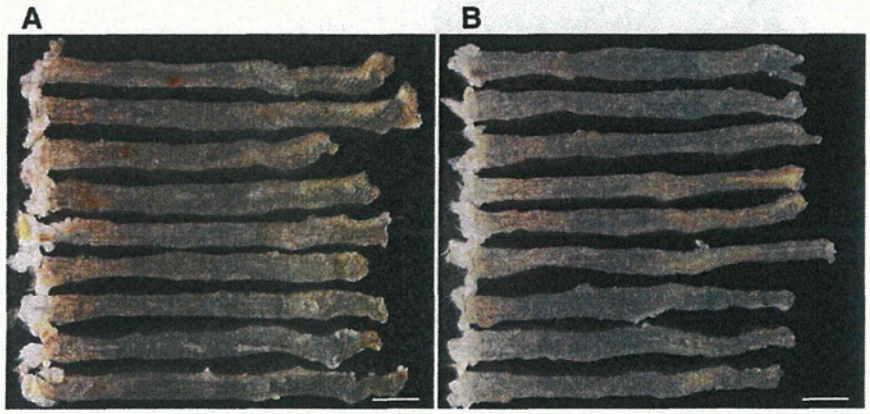

Figure 4 Macroscopic view of large bowel. Macroscopic view of large bowel of KAD rats that were not given 5-FU (**A**) and that were given 50 mg/kg 5-FU (**B**). Colon tumors that developed in both groups were mainly distributed in the rectum and distal colon, which was assumed to be within 8 cm from the anus. No tumors were observed in the proximal colon. Left side: anus. Right side: cecum. Bar: 2 cm.

Table 1 Effects of 5-FU on the development of colon tumors in the KAD rat

Treatment	No. of rats	Macroscopic observation		Microscopic observation			
		Multiplicity	Volume (mm^3)[1]	Multiplicity			Volume (mm^3)[2]
				adenomas	adenocarcinomas	total	adenocarcinoma
Saline	9	5.56 ± 3.43	106.34 ± 68.92	3.11 ± 2.52	3.22 ± 2.77	6.33 ± 4.87	63.85 ± 51.06
50 mg/kg 5-FU	9	6.33 ± 3.04	77.28 ± 57.23	3.78 ± 1.79	2.33 ± 1.94	6.11 ± 2.37	34.40 ± 31.26 [3]

[1]Tumor volume was determined by the formula $V = a \times b^2/2$ (V: volume. a: the largest superficial diameter and b: the smallest superficial diameter).
[2]Volumes of adenomas were too small to calculate.
[3]Adenocarcinoma volumes observed in the 5-FU-treated KAD rats were significantly reduced as compared with those of non-treated rats ($p < 0.02$).

the number of tumors observed by the endoscopy is correlated to the volume of tumors obtained by the microscopy at week 8. We, therefore, recommend counting the number of tumors using endoscopic observation before dividing the rats into groups.

It is important to identify biomarkers that are used to predict efficacy and safety of anti-tumor drugs. Rats can be subjected to the sequential sampling of bloods. The amounts of bloods or urines are enough to be examined. Moreover, drug kinetics can be monitored by *in vivo* imaging [14]. Thus, the chemotherapeutic bioassay with the KAD rats is a candidate system to explore the biomarkers.

5-FU is a pyrimidine analog and when incorporated into DNA inhibits the cell's ability to synthesize DNA. Eventually 5-FU induces cell cycle arrest and apoptosis, mainly in cells with high proliferative activity such as cancer cells [15]. Side effects of 5-FU, such as diarrhea and weight loss, are problematic in performing chemotherapeutic tests with animal models. Thus, it is important to determine the maximum tolerated dose (MTD) that does not produce profound weight loss, and that causes no drug-related lethality. Usually the MTD of 5-FU in rats ranges from 25 to 100 mg/kg, depending on the 5-FU administration schedules [16]. In the current study, we found that the MTD was 50 mg/kg of 5-FU when administered to tumor-bearing KAD rats by i.v. injection. Although the MTD should be determined using different administration schedules and routes, the MTD that we determined in the present study can be a helpful guide in setting doses of anti-cancer drugs in further chemotherapeutic tests with KAD rats.

In our study, the treatment of tumor-bearing KAD rats with 5-FU failed to reduce the multiplicity of adenoma or adenocarcinoma. However, the treatment significantly reduced adenocarcinoma tumor volume and cell proliferation as well as increased adenocarcinoma apoptosis, which was consistent with the mode of action of the 5-FU [15]. Treatment response assessed in terms of

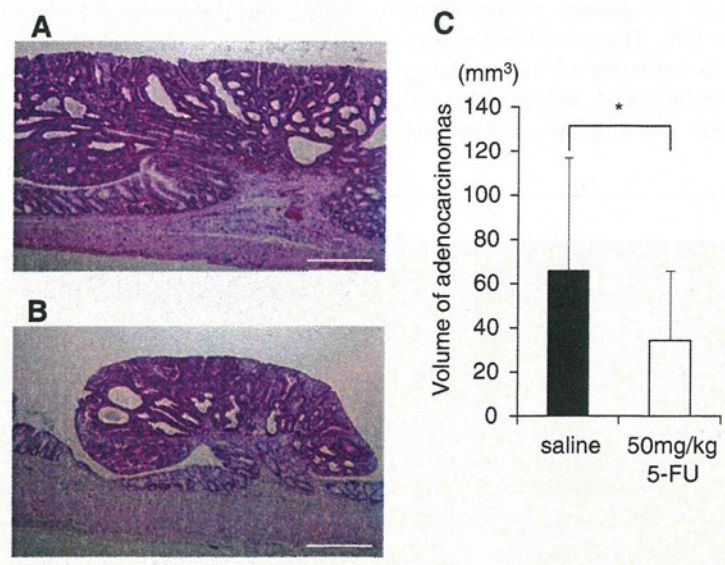

Figure 5 Histopathological analysis of colonic adenocarcinomas. Colonic adenocarcinoma developed in KAD rats that were not given 5-FU (**A**) and that were given 50 mg/kg 5-FU (**B**). Most of the adenocarcinomas in KAD rats that received 50 mg/kg 5-FU were smaller than those in the control group (hematoxylin and eosin stain). Bar: 500 μm. (**C**) Average volume of adenocarcinoma tumors grown in KAD rats that were given saline or 5-FU (50 mg/kg). The mean volume of adenocarcinoma tumors in the 5-FU-treated rats were significantly smaller than those in the non-treated rats. *: $p < 0.02$.

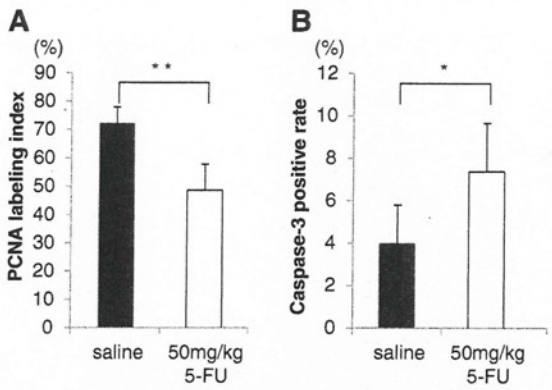

Figure 6 Cell proliferation and apoptosis in adenocarcinomas of the 5-FU treated KAD rats. (**A**) The PCNA labeling index was significantly lower in the 5-FU treated KAD rats (50 mg/kg) than that in the control KAD rats, indicating significant decrease in cell proliferation in the adenocarcinomas. **: $p < 0.001$. (**B**) The cleaved caspase-3 positive rate was significantly higher in the 5-FU treated KAD rats (50 mg/kg) than that in the control KAD rats, indicating significant increase in apoptosis in the adenocarcinomas. *: $p < 0.02$.

change in tumor size after 5-FU administration in the present study amounted to a 30% reduction, which was similar to the response rate of 5-FU as a single agent seen in human cancers, including CRC [17]. These findings indicated that the response of tumors in AOM/DSS-treated KAD rats to 5-FU treatment was similar to human CRC, and supported the view that this should be a useful bioassay system for employment in further chemotherapeutic studies.

Conclusions

In the present study we established a chemotherapeutic bioassay system for CRC using KAD rats. In this system, we could set the experimental groups on the basis of the number of tumors detected by endoscopic examination. After 5-FU administration rat colon tumors induced by AOM/DSS treatments showed a similar response, in terms of percentage reduction in size and cell proliferation and percentage elevation in apoptosis, to those reported in clinical CRC studies. Thus, we expect that this system could effectively promote the development of new anti-tumor drugs and regimens for human CRC.

Additional files

Additional file 1: Table S1. Number and total volume of tumors found in KAD rats at week 8.

Additional file 2: Figure S1. The correlation of total volume of tumors with the numbers of polypoid lesions observed by endoscopy at Week8. Regression formula was made with Excel software package (Microsoft). Vertical axis was shown in logarithmic scale.

Competing interests

The authors declare that they have no competing interests.

Authors' contributions

KY and TK conceived the study and designed the experiments. KY, TH, YN and KH performed the experiments. TT performed the histopathological analysis. KY, TK and TT wrote the manuscript. TS revised the manuscript. All authors have read and approved the final manuscript.

Acknowledgments

This work was supported in part by a Grant-in-Aid for Cancer Research from the Ministry of Health, Labour and Welfare (to TK), and Grants-in-Aid for Scientific Research from the Japan Society for the Promotion of Science (21300153 to TK and 0233639 to KY). The KAD (F344-*Apc*^{m1Kyo}) rat has been deposited in the National BioResource Project-Rat in Japan and is available from the Project (http://www.anim.med.kyoto-u.ac.jp/nbr).

Author details

[1]Institute of Laboratory Animals, Graduate School of Medicine, Kyoto University, Yoshidakonoe-cho, Sakyo-ku, Kyoto 606-8501, Japan. [2]Sunplanet Co., Ltd, 4388 Makita, Kamiishizu, Ogaki 503-1602, Japan. [3]Cancer Research and Prevention, The Tohkai Cytopathology Institute, 4-33 Minami-Uzura, Gifu 500-8285, Japan.

Received: 24 April 2012 Accepted: 26 September 2012
Published: 3 October 2012

References

1. Blumenthal RD, Osorio L, Hayes MK, Horak ID, Hansen HJ, Goldenberg DM: **Carcinoembryonic antigen antibody inhibits lung metastasis and augments chemotherapy in a human colonic carcinoma xenograft.** *Cancer Immunol Immunother* 2005, **54**(4):315–327.
2. Corpet DE, Pierre F: **Point: From animal models to prevention of colon cancer. Systematic review of chemoprevention in min mice and choice of the model system.** *Cancer Epidemiol Biomarkers Prev* 2003, **12**(5):391–400.
3. Williams KJ, Telfer BA, Stratford IJ, Wedge SR: **ZD1839 ('Iressa'), a specific oral epidermal growth factor receptor-tyrosine kinase inhibitor, potentiates radiotherapy in a human colorectal cancer xenograft model.** *Br J Cancer* 2002, **86**(7):1157–1161.
4. Ding Y, Cravero JD, Adrian K, Grippo P: **Modeling pancreatic cancer *in vivo*: from xenograft and carcinogen-induced systems to genetically engineered mice.** *Pancreas* 2010, **39**(3):283–292.
5. Voskoglou-Nomikos T, Pater JL, Seymour L: **Clinical predictive value of the *in vitro* cell line, human xenograft, and mouse allograft preclinical cancer models.** *Clin Cancer Res* 2003, **9**(11):4227–4239.
6. Femia AP, Caderni G: **Rodent models of colon carcinogenesis for the study of chemopreventive activity of natural products.** *Planta Med* 2008, **74**(13):1602–1607.
7. Bruce WR: **Counterpoint: From animal models to prevention of colon cancer. Criteria for proceeding from preclinical studies and choice of models for prevention studies.** *Cancer Epidemiol Biomarkers Prev* 2003, **12**(5):401–404.
8. Reddy BS: **Studies with the azoxymethane-rat preclinical model for assessing colon tumor development and chemoprevention.** *Environ Mol Mutagen* 2004, **44**(1):26–35.
9. Reddy BS, Maeura Y: **Tumor promotion by dietary fat in azoxymethane-induced colon carcinogenesis in female F344 rats: influence of amount and source of dietary fat.** *J Natl Cancer Inst* 1984, **72**(3):745–750.
10. Tanaka T, Kohno H, Suzuki R, Yamada Y, Sugie S, Mori H: **A novel inflammation-related mouse colon carcinogenesis model induced by azoxymethane and dextran sodium sulfate.** *Cancer Sci* 2003, **94**(11):965–973.
11. Yoshimi K, Tanaka T, Takizawa A, Kato M, Hirabayashi M, Mashimo T, Serikawa T, Kuramoto T: **Enhanced colitis-associated colon carcinogenesis in a novel Apc mutant rat.** *Cancer Sci* 2009, **100**(11):2022–2027.
12. Carlsson G, Gullberg B, Hafstrom L: **Estimation of liver tumor volume using different formulas - an experimental study in rats.** *J Cancer Res Clin Oncol* 1983, **105**(1):20–23.
13. Hanahan D, Weinberg RA: **The hallmarks of cancer.** *Cell* 2000, **100**(1):57–70.
14. Ogawa K, Mukai T, Kawai K, Takamura N, Hanaoka H, Hashimoto K, Shiba K, Mori H, Saji H: **Usefulness of competitive inhibitors of protein binding for**

improving the pharmacokinetics of 186Re-MAG3-conjugated bisphosphonate (186Re-MAG3-HBP), an agent for treatment of painful bone metastases. *Eur J Nucl Med Mol Imaging* 2009, **36**(1):115–121.
15. Thomas DM, Zalcberg JR: **5-fluorouracil: a pharmacological paradigm in the use of cytotoxics.** *Clin Exp Pharmacol Physiol* 1998, **25**(11):887–895.
16. Cao S, Rustum YM: **Synergistic antitumor activity of irinotecan in combination with 5-fluorouracil in rats bearing advanced colorectal cancer: role of drug sequence and dose.** *Cancer Res* 2000, **60**(14):3717–3721.
17. Salonga D, Danenberg KD, Johnson M, Metzger R, Groshen S, Tsao-Wei DD, Lenz HJ, Leichman CG, Leichman L, Diasio RB, *et al*: **Colorectal tumors responding to 5-fluorouracil have low gene expression levels of dihydropyrimidine dehydrogenase, thymidylate synthase, and thymidine phosphorylase.** *Clin Cancer Res* 2000, **6**(4):1322–1327.

doi:10.1186/1471-2407-12-448
Cite this article as: Yoshimi *et al.*: Use of a chemically induced-colon carcinogenesis-prone *Apc*-mutant rat in a chemotherapeutic bioassay. *BMC Cancer* 2012 **12**:448.

The American Journal of Pathology, Vol. 182, No. 4, April 2013

ELSEVIER

The American Journal of
PATHOLOGY

ajp.amjpathol.org

GASTROINTESTINAL, HEPATOBILIARY, AND PANCREATIC PATHOLOGY

Tumor Suppressor APC Protein Is Essential in Mucosal Repair from Colonic Inflammation through Angiogenesis

Kazuto Yoshimi,* Takuji Tanaka,† Tadao Serikawa,* and Takashi Kuramoto*

From the Institute of Laboratory Animals, Graduate School of Medicine, Kyoto University, Kyoto; and Cancer Research and Prevention,† The Tohkai Cytopathology Institute, Gifu, Japan*

Accepted for publication December 24, 2012.

Address correspondence to Takashi Kuramoto, Ph.D., Institute of Laboratory Animals, Graduate School of Medicine, Kyoto University, Yoshidakonoe-cho, Sakyo-ku, Kyoto 606-8501, Japan. E-mail: tkuramot@anim.med.kyoto-u.ac.jp.

Mucosal repair after acute colonic inflammation is central to maintaining mucosal homeostasis. Failure of mucosal repair often leads to chronic inflammation, sometimes associated with inflammatory bowel disease (IBD). The adenomatous polyposis coli (*APC*) tumor suppressor gene regulates the Wnt signaling pathway, which is essential for epithelial development, and inactivation of *APC* facilitates colorectal cancer. Our previous study suggested that *APC* is involved in pathogenesis of colonic inflammation; however, its role in mucosal repair remains unknown. In this article, we report that colitis induced by dextran sodium sulfate persisted with delayed mucosal repair in Kyoto Apc Delta (KAD) rats lacking the APC C terminus. Defects in the repair process were accompanied by an absence of a fibrin layer covering damaged mucosa and reduced microvessel angiogenesis. APC was up-regulated in vascular endothelial cells (VECs) in inflamed mucosa in KAD and F344 (control) rats. The VECs of KAD rats revealed elevated cell adhesion and low-branched and short-length tube formation. We also found that DLG5, which is associated with IBD pathogenesis, was up-regulated in VECs in inflamed mucosa and interacted with the C terminus of APC. This finding suggests that loss of interaction between the APC C terminus and DLG5 affects VEC morphology and function and leads to persistence of colitis. Therefore, APC is essential for maintenance of intestinal mucosal homeostasis and can consequently contribute to IBD pathogenesis. *(Am J Pathol 2013, 182: 1263–1274; http://dx.doi.org/10.1016/j.ajpath.2012.12.005)*

Mucosal epithelial defense is an important system to prevent injuries induced by undigested substances, acid, ischemia, and microbial infection.[1,2] Once the mucosa is injured, the repair process—which is complex but primarily consists of the immune response, granulation tissue formation, angiogenesis, and epithelial regeneration—plays a central role to prevent further injuries.[3] Defects in such repair systems are a potential risk for persistent inflammation of the intestine or colon, which can lead to chronic inflammation, such as that seen in inflammatory bowel disease (IBD).

IBD, including ulcerative colitis and Crohn's disease, represents a chronic, relapsing and remitting inflammatory condition that affects individuals throughout life.[4] Patients with IBD are at risk of developing colorectal cancer.[5] Although it is widely accepted that genetic, environmental, and immunologic factors are involved,[6,7] the pathogenesis of IBD remains unclear. No completely effective therapeutic strategy has yet been established.

To investigate the pathogenesis of IBD, animal models of experimental colitis have been developed.[8] The dextran sodium sulfate (DSS) model is excellent for its resemblance to the clinical symptom of the IBD and for its ease of reproducibility and accessibility.[9] Providing drinking water containing DSS for several days induces colitis in rodents, which has characteristics similar to human ulcerative colitis, such as signs of diarrhea, gross rectal bleeding, weight loss, shortening of the colorectum, histologic features of multiple erosions, and inflammatory mucosal changes, occasionally including crypt abscess. Colitis is also predominant in the

Supported in part by a Grant-in-Aid for Cancer Research from the Ministry of Health, Labour and Welfare and Grants-in-Aid for Scientific Research from the Japan Society for the Promotion of Science (21300153 to T.K. and 0233639 to K.Y.).

The KAD (F344-*Apc*^{m1Kyo}) rat has been deposited in the National Bioresource Project-Rat in Japan (Institute of Laboratory Animals, Kyoto University).

http://dx.doi.org/10.1016/j.ajpath.2012.12.005

descending and sigmoid colons and the rectum and associated with alteration of intestinal flora. Some pathogenic and regulatory factors demonstrated in the DSS model, such as cytokines, growth factors, and inflammatory enzymes, have been exploited to develop future therapeutic strategies against IBD.[8]

Adenomatous polyposis coli (*APC*) has been identified as the causative gene of familial adenomatous polyposis of the colon, which is characterized by numerous polyps in the intestine.[10] Genetic studies using mutant mouse models indicate that *APC* is essential for development and that its inactivation facilitates tumorigenesis.[11]

APC is a 2843—amino acid polypeptide and is composed of multiple domains. Via these domains, APC can bind to various proteins, including the guanine-nucleotide-exchange factor ASEF1, the Wnt pathway component β-catenin, microtubules (MTs), the cytoskeletal regulator EB1, and homologs of the *Drosophila* disks large protein (DLG).[12] Most cancer-linked *APC* mutations occur at the central region of *APC* (the so-called mutation cluster region) and result in truncation of almost half of the C terminal region of the protein.[13] Because these truncations cause loss of the domains required for binding to β-catenin, MTs, EB1, and DLG, the interaction of APC with these molecules has been considered essential for its tumor-suppressing activity.

In 1999, Smits et al[14] developed a knockout mouse that carried a targeted mutation at codon 1638, *Apc*1638T (T for truncated). The resultant truncated APC protein contains β-catenin binding sites but lacks all of the C-terminus domains. $Apc^{1638T/1638T}$ mice survive to adulthood and are tumor free. Thus, the interaction of APC with β-catenin but not MTs, EB1, or DLG is critical in tumorigenesis. In addition, $Apc^{1638T/1638T}$ mice have growth retardation, reduced postnatal viability, the absence of preputial glands, and the formation of nipple-associated cysts.[14] Enlarged thyroid follicles and low responsiveness to thyroid-stimulating hormone are also found with $Apc^{1638T/1638T}$ mice.[15] Therefore, the C terminus of APC appears to be involved in the development of several tissues as described in this article; however, its physiologic function *in vivo* remains unclear.

We recently developed a mutant rat that carries a homozygous nonsense mutation at codon 2523 ($Apc^{\Delta 2523}$), which we call the Kyoto Apc Delta (KAD) rat.[16] The KAD rat expresses truncated APC protein that contains β-catenin binding sites but lacks the C terminus (321 amino acids in length), which can bind to MT, EB1, and DLG. KAD rats survive to adulthood and are free of intestinal tumors. However, when KAD rats received a single subcutaneous administration of 20 mg/kg of azoxymethane and 1 week later were given 2% DSS (in drinking water) for 1 week, they had a significantly higher incidence and multiplicity of colon tumors at week 15 compared with control F344 rats.[16,17] In contrast, KAD rats treated with azoxymethane only did not develop colon tumors (as assessed by the carcinogenesis test) by 15 weeks, similar to the azoxymethane-treated F344 rats. These findings suggest that the KAD rat is susceptible to inflammation provoked by the colitis-inducing agent and that the C terminus of APC appears to be involved in the pathogenesis of colitis.

In this study, we found that loss of the C terminus of APC affected the morphology and function of vascular endothelial cells (VECs) and led to a persistence of colitis. Our results reveal a new role of APC in the angiogenesis associated with mucosal repair of damage due to colitis.

Materials and Methods

Rats

F344/NSlc and KAD (homozygous for the $Apc^{\Delta 2523}$ mutation, official strain name: F344-Apc^{m1Kyo}) rats were obtained from Japan SLC, Inc. (Hamamatsu, Japan). KAD rats were backcrossed five times with female F344/NSlc rats to remove latent mutations induced by N-ethyl N-nitrosourea.[16] The rats were kept at the Institute of Laboratory Animals, Graduate School of Medicine, Kyoto University, under conditions of 50% humidity and a 14:10-hour light:dark cycle. They were fed a standard pellet diet (F-2, Oriental Yeast Co., Ltd, Tokyo, Japan) and tap water *ad libitum*.

Induction of Colitis

Male KAD rats ($n = 30$) and control F344/NSlc rats (F344 rats, $n = 30$) aged 5 weeks were given 2% DSS (molecular weight = 36,000-50,000 kDa) (MP Biochemicals, LLC., Solon, OH) in their drinking water for 1 week. The rats were divided into three groups: those sacrificed immediately after DSS treatment (week 1), those sacrificed 1 week after terminating the treatment (week 2), and those sacrificed 3 weeks after the treatment (week 4). The animals were sacrificed by cervical dislocation under anesthesia with isoflurane (Mylan Inc., New York, NY). The experimental procedures were approved by the Animal Research Committee of Kyoto University and were performed according to the Regulations on Animal Experimentation of Kyoto University.

Clinical assessment of inflammation involved monitoring the body weight and scoring the diarrhea and fecal blood for each rat.[18] The presence of diarrhea and fecal blood were scored on a scale of 1 and 2, respectively. The clinical inflammatory score for each animal was obtained by adding the diarrhea and fecal blood scores.

Histopathologic Analysis

An hour prior to sacrifice, the rats were injected intraperitoneally with 50 mg/kg of 5-bromo-2′-deoxyuridine (BrdU; Sigma, St. Louis, MO) to permit immunohistochemical (IHC) analysis of BrdU. On autopsy, the colorectum of each rat was resected and gently washed with PBS to remove feces. Half was used for a RT-PCR assay, and the other was fixed in 10% buffered formalin and embedded in paraffin for histopathologic analysis. Five serial sections of colonic

tissues (3 μm thick) were made: two sections stained with H&E to permit histologic examination and with phosphotungstic acid hematoxylin (PTAH) for detection of fibrin. Other sections were used for IHC with an LSAB2 Kit (Dako, Glostrup, Denmark). Anti-APC monoclonal antibody (EP701Y; Abcam, Cambridge, UK) and anti-CD31/platelet–endothelial cell adhesion molecule 1 polyclonal antibody (Santa Cruz Biotechnology, Santa Cruz, CA) were used as primary antibodies.

Cell proliferation in the inflamed mucosa was accessed by determination of the labeling index for BrdU-positive cells. The number of BrdU-positive cells was counted in at least 20 well-oriented crypts for each group. The labeling index was calculated by dividing the number of BrdU-positive cells by the total number of nucleated cells for each well-oriented crypt.

To investigate the localization of EB1, DLG1, and DLG5 in the inflamed colon, fluorescent immunochemistry was performed. Anti-CD31 polyclonal antibody (Santa Cruz Biotechnology) and anti-EB1, anti-DLG1, and anti-DLG5 polyclonal antibodies (Abcam) were used as primary antibodies. Alexa Fluor 488–conjugated anti-rabbit IgG antibody and Alexa Fluor 594–conjugated anti-mouse IgG antibody (1:200; Invitrogen, Carlsbad, CA) were used as secondary antibodies. Immunostained sections were visualized using a Biorevo immunofluorescence microscope (Keyence, Osaka, Japan).

Analysis of Colonic Microvasculature Density

Vascular density was calculated using an international consensus method to quantify angiogenesis, as previously described.[19] Briefly, CD31-stained distal colonic sections were scanned and the number of vessels within the mucosa was counted to identify the most vascularized area. Vascular density per field was obtained from at least five microphotographs of the most vascularized mucosa for each rat. Quantitative analysis of the data was performed using WinROOF software version 6.0 (Mitani Corp., Fukui, Fukui, Japan).

Real-Time PCR

Total RNA was isolated from inflamed mucosa of the distal colon 3 cm from the anus, and cDNA was synthesized. Real-time RT-PCR was performed using a Thermal Cycler Dice Real Time System with SYBR Premix Ex TaqII (Takara Bio Inc., Otsu, Shiga, Japan). The primers used were: *Tnfa*, 5′-AACTCGAGTGACAAGCCCGTAG-3′ and 5′-GTACCAC-CAGTTGGTTGTCTTTGA-3′; *Il1b*, 5′-GCTGTGGCAGC-TACCTATGTCTTG-3′ and 5′-AGGTCGTCATCATCCCA-CGAG-3′; *Il10*, 5′-CAGACCCACATGCTCCGAGA-3′ and 5′-CAAGGCTTGGCAACCCAAGTA-3′; *Ptgs2*, 5′-GCGA-CTGTTCCAAACCAGCA-3′ and 5′-TGGGTCGAACTTG-AGTTTGAAGTG-3′; *Ptges*, 5′-TACGCGGTGGCTGTCA-TCA-3′ and 5′-CTCCACATCTGGGTCACTCCTG-3′; *Ppia*, 5′-GGCAAATGCTGGACCAAACAC-3′ and 5′-AAACGC-TCCATGGCTTCCAC-3′. The number of target molecules was normalized against those of *Ppia* as an internal control.[20]

Reporter Gene Assay of Wnt Signaling

To measure Wnt signaling activity, rat embryonic fibroblasts (REFs) were isolated from E12.5 embryos of F344 and KAD rats in Dulbecco's modified Eagle's medium supplemented with 10% fetal bovine serum. REFs were then plated on 24-well culture plates 24 hours before transfection. Lipofectamine LTX (Invitrogen) was used to co-transfect REFs with pTOPFLASH or pFOPFLASH vector (Millipore, Billerica, MA) and pSV-β-Gal vector (Promega Corp., Madison, WI) as an internal control according to the manufacturer protocol. Cells in half of the plates were stimulated with 150 ng/mL of Wnt3a (R&D Systems Inc., Minneapolis, MN) 3 hours later. Luciferase activities were measured 24 hours after transfection with Luciferase Assay Systems (Promega).

Isolation of VECs

VECs were isolated from the thoracic aorta of four F344 and four KAD rats aged 8 weeks, as described previously.[21] VECs were cultured in MCDB 131 medium supplemented with epidermal growth factor, endothelial cell growth supplements, vascular endothelial growth factor, hydrocortisone, heparin, and 2% fetal bovine serum. Almost all cultured cells were of endothelial origin, as assessed by staining with Dil-Ac-LDL (Biomedical Technologies Inc., Stoughton, MA). All VECs were examined twice in all *in vitro* experiments to confirm their reproducibility.

Immunofluorescence Microscopy

Cells cultured on collagen-coated coverslips were fixed with 4% paraformaldehyde at 37°C for 15 minutes. After permeabilization and a blocking reaction, they were incubated with antibodies against N-terminal APC (H-290; Santa Cruz), C-terminal APC (C-20; Santa Cruz), α-tubulin (YL1/2; Abcam), paxillin (Abcam), and EB1 (Abcam). They were then treated with Alexa Fluor–conjugated secondary antibodies and phalloidin (Invitrogen), followed by staining with DAPI.

In Vitro Proliferation, Migration, Adhesion, and Tube Formation Assay

A BrdU incorporation assay was performed using the BrdU Labeling and Detection Kit III (Roch Diagnostics GmbH, Mannheim, Germany), according to the manufacturer protocol. Briefly, VECs were plated and labeled with 100 μmol/L BrdU for 6 hours. Cells were stained with the anti–BrdU-POD antibody and quantified by measuring absorbance with an enzyme-linked immunosorbent assay (ELISA) reader. The migration activity of VECs was measured using a wound healing assay, as described

previously.[22] Microscopic images were captured at 0 and 16 hours after culture, and the percentage of migrated area was quantified. The adhesion activity of the VECs was measured using a wash assay, as described previously.[23] For tube formation assay, the VECs were plated onto a layer of Matrigel (BD Biosciences, Franklin Lakes, NJ) and incubated at 37°C for 24 hours. Microphotographs of the formation of the capillary-like networks were obtained from at least four fields. Quantitative analyses of their tube length and the number of branching points were performed using WinROOF software version 6.0.

Plasmids

FLAG-tagged rat APC C-terminus (FLAG-APC-C-term), V5-tagged DLG1 and DLG5 plasmids were constructed. Briefly, the coding sequences of rat APC, DLG1, and DLG5 were amplified from brainstem cDNAs of F344/NSlc rats using KOD Plus Neo DNA polymerase (Toyobo, Osaka, Japan). APC C-terminus cDNA (321 amino acids) was cloned into the p3xFLAG-CMV-7.1 vector (Sigma). DLG1 and DLG5 cDNAs were cloned into the pcDNA6.2/V5/GW/D-TOPO vector using a TOPO Expression kit (Invitrogen). To increase efficiency of transfection, the truncated DLG5 cDNAs were cloned. The sequences of PCR primers to amplify the cDNAs are as follows: FLAG-APC-C-term, 5′-CATCTAGCGGCCGCCTCAAAGCGGCATGATATCG-CACGCTCCCATTCTG-3′ and 5′-CTTTCTGGATCCTT-TAAACAGACGTCACGAGGTAAGACCCAGAATGG-3′; DLG1-V5, 5′-CACCATGCCGGTCCGGAAGCAAGATA-CCCAGAGA-3′ and 5′-TAATTTTTCTTTTGCTGGGAC-CCAGATGTAAGGACC-3′; DLG5-V5, 5′-CACCATGGA-GCCGCAGCGCCGGGAGCTGCTCGCC-3′ and 5′-GGG-TGGGCAAGCGGGTATCCACAGGACTTT-3′; DLG5-1-V5, 5′-CACCATGGAGCCGCAGCGCCGGGAGCTGCT-CGCC-3′ and 5′-TTCCATTTGCTCCTTGAGTTCTTTA-3′; DLG5-2-V5, 5′-CACCTGTCAGCTGGAGAAGGAGGC-3′ and 5′-TGAGGTCTGAGGCTGGCTACAGAAG-3′; and DLG5-3-V5, 5′-CACCATGGGCTCTGACAGAGGCTCA-3′ and 5′-GGGTGGGCAAGCGGGTATCCACAGGACT-TT-3′. All constructs were verified by sequence analysis.

Co-Immunoprecipitation Assay

A co-immunoprecipitation assay was performed to examine binding reactivity of the C terminus of APC to DLG1 and DLG5. The recombinant V5-tagged rat DLG1 and DLG5 proteins were generated by human cervical cancer cells (Hela cells). Hela cells were cultured in Dulbecco's modified Eagle's medium (Life Technologies, Grand Island, NY) supplemented with 10% fetal bovine serum under an atmosphere of 95% oxygen and 5% carbon dioxide at 37°C. Hela cells were co-transfected with FLAG-APC-C-term plasmids and DLG1-V5, DLG5-V5, DLG5-1-V5, DLG5-2-V5, or DLG5-3-V5 plasmids using Lipofectamine LTX (Invitrogen). As a negative control, p3xFLAG-CMV-7.1 vector was used. The cells were lysed with Triton X-100 lysis buffer after incubation for 18 hours. The recombinant FLAG-APC-C-term proteins were purified and collected by immunoprecipitation using a FLAG Immunoprecipitation Kit (Sigma). As a positive control, FLAG-BAP fusion protein was used. The resulting supernatants were subjected to immunoblot analysis as described previously.[16] The primary antibodies were rabbit anti-EB1 monoclonal antibody (1:1000, Abcam), mouse anti-V5 monoclonal antibody (1:5000, Invitrogen), and mouse anti-FLAG M2 monoclonal antibody (1:5000, Sigma). The secondary antibodies were

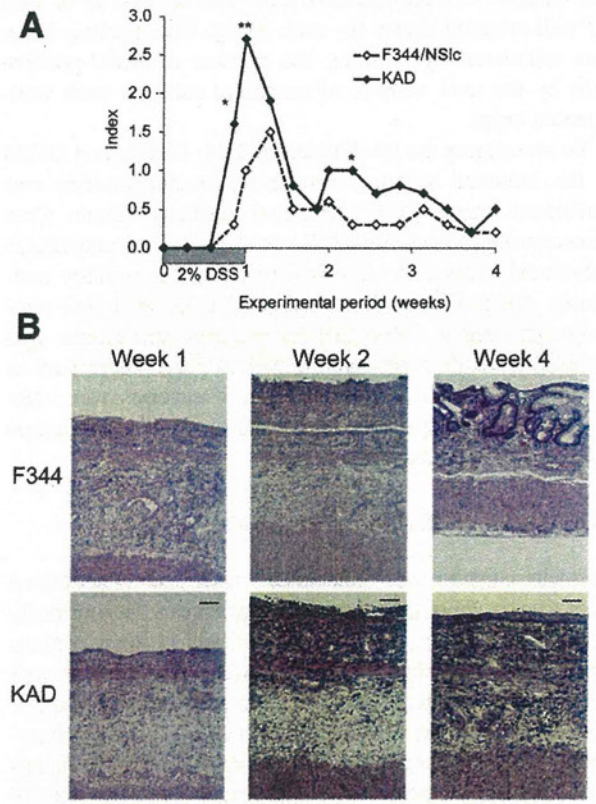

Figure 1 Sustained colon inflammation by DSS in the C terminus of APC-deficient rats. **A:** Clinical inflammatory scores for KAD and F344 rats that received 2% DSS in drinking water. The severity of inflammation was assessed by clinical scoring for diarrhea and fecal blood. $*P < 0.05$, $**P < 0.02$. **B:** Histologic sections of representative distal colonic lesions of F344 and KAD rats that received drinking water that contained 2% DSS. Pictures were obtained from F344 and KAD rats immediately after terminating DSS exposure (week 1), 1 week after terminating DSS exposure (week 2), and 3 weeks after terminating DSS treatment (week 4). Note mucosal denudation, crypts loss, and diffuse and marked infiltration of inflammatory cells, including polymorph neutrophils, plasma cells, and lymphocytes throughout the lamina propria and submucosa at weeks 1 and 2. At week 1, eosinophilic structures covering the damaged mucosa were observed for F344 but not for KAD rats. At week 4, the mucosal ulcer had healed by crypt degeneration accompanied by fibrosis and a diminished number of inflammatory cells in the F344 rats. However, mucosal ulcers accompanied by diffuse and marked inflammatory cell infiltrate, edema, and dilated small vessels were observed in the lamina propria and submucosa of the distal colon of KAD rats. In some KAD rats, elongation of squamous epithelium was seen on ulcerated mucosa. H&E staining. Original magnification ×200. Scale bar = 100 μm.

Table 1 Expression Levels of Inflammatory Cytokines in KAD Rats

	Week 0		Week 1		Week 2		Week 4	
Gene	KAD	F344/NSlc	KAD	F344/NSlc	KAD	F344/NSlc	KAD	F344/NSlc
Tnfα	1.26 ± 0.91	1.84 ± 1.53	0.47 ± 1.10	0.25 ± 0.30	88.93 ± 236.33	9.19 ± 11.50	3.24 ± 3.76*	0.22 ± 0.36
Il1β	0.24 ± 0.11	0.49 ± 0.32	118.08 ± 153.51	26.20 ± 33.14	927.33 ± 1204.49	889.79 ± 1233.85	110.61 ± 148.11*	4.70 ± 6.62
Il10	0.02 ± 0.01	0.04 ± 0.03	1.19 ± 1.59	0.26 ± 0.29	2.62 ± 4.37	3.17 ± 2.77	0.65 ± 0.77*	0.05 ± 0.05
Ptgs2/Cox2	0.75 ± 0.37	0.98 ± 0.18	0.34 ± 0.32	0.61 ± 0.77	186.45 ± 344.84	39.82 ± 101.57	13.66 ± 18.92*	0.16 ± 0.23
Ptges	0.62 ± 0.25	0.44 ± 0.46	13.14 ± 21.22	1.11 ± 1.56	73.20 ± 90.45	58.30 ± 77.77	11.49 ± 12.06*	2.18 ± 2.47

*$P < 0.05$.

horseradish peroxidase–conjugated anti-mouse and anti-rabbit IgG (1:2000, Sigma). Immunoblotted proteins were visualized using an ECL select Western blotting detection system (GE Healthcare, Piscataway, NJ).

Statistical Analysis

Student's *t*-test was performed, and SDs were calculated using the statistics package in Microsoft Excel (Microsoft Inc., Redmond, WA). $P < 0.05$ was considered statistically significant.

Results

KAD Rats Display Severe Acute Colitis and Sustained Colonic Inflammation

DSS can effectively induce colonic inflammation in rats, and a loss of body weight, diarrhea, and fecal blood are observed as the clinical symptoms.[24] Loss of body weight was noted from day 8 to day 10 in both F344 and KAD rats; however, there were no differences between the two strains of rat. There were no differences in water and food consumption during exposure to DSS (data not shown). KAD rats obtained higher inflammatory scores, mainly resulting from watery diarrhea and visible fecal blood, compared with F344 rats during exposure to DSS. This finding was true even after terminating exposure to DSS (Figure 1A).

Macroscopically, severe inflammation was generally located in the distal colon of the F344 and KAD rats. Prominent macroscopic features of KAD rat colon were dilation, primarily the distal part of the colon (one-third of the colon from the anus), thickening of the colonic wall, and extensive loss of the mucosa accompanied by bleeding. These findings were also observed in F344 rats, but the severity was less than that of KAD rats. The changes in KAD rats lasted until week 4; in F344 rats they lasted until week 2, and this was associated with their clinical symptoms.

Histopathologic analysis revealed the presence of mucosal ulceration, crypt loss, diffuse inflammatory cell infiltrate of the lamina propria and submucosa, debris, exudates, edema, and congestion and dilatation of the capillary blood vessels in the affected colons of both F344 and KAD rats at weeks 1 and 2 (Figure 1B). Of note, at week 1, eosinophilic structures covering the damaged mucosa were observed in F344 rats, whereas few structures

Table 2 Labeling Index Observed for DSS-Treated Colonic Mucosa

Week	F344	KAD
2	14.1 ± 7.9	16.1 ± 6.7
4	4.1 ± 1.5	8.5 ± 4.0*

The labeling index was calculated by dividing the number of BrdU-positive cells by the total number of nucleated cells per well-oriented crypt.
*$P < 0.001$ compared with F344 rats.

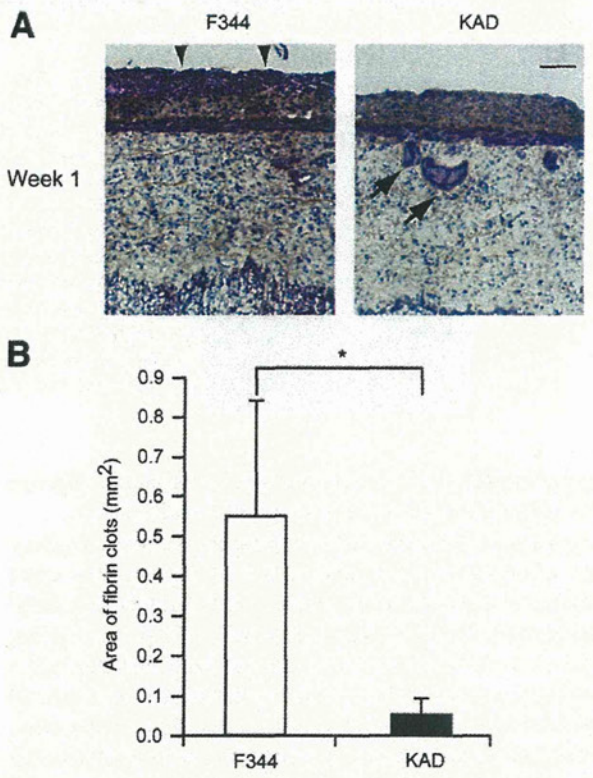

Figure 2 Lack of fibrin clot formation along the mucosal ulcer in the colon of KAD rats. **A:** PTAH-stained sections of F344 and KAD rats at week 1. Fibrin pseudo-membrane covering the surface of the damaged mucosal epithelia was observed in F344 rat colon (**arrowheads**). Fibrin pseudo-membranes were absent on the colonic mucosa of KAD rats; instead, fibrin microthrombi were observed beneath the lamina propria (**arrows**). Scale bar = 100 μm. **B:** The area of fibrin layers covering the surface of DSS-induced inflamed mucosa per rat. *$P < 0.001$.

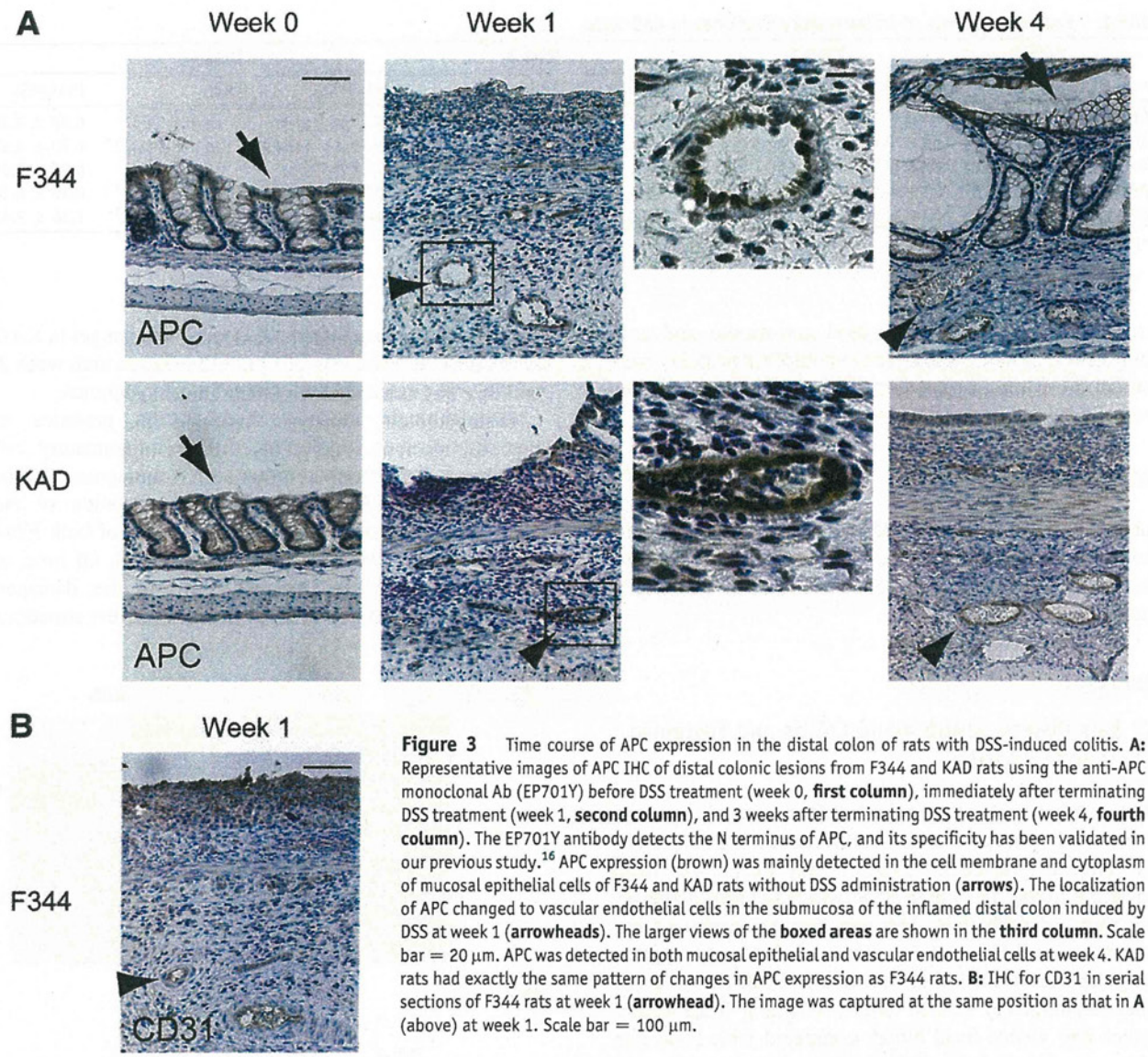

Figure 3 Time course of APC expression in the distal colon of rats with DSS-induced colitis. **A:** Representative images of APC IHC of distal colonic lesions from F344 and KAD rats using the anti-APC monoclonal Ab (EP701Y) before DSS treatment (week 0, **first column**), immediately after terminating DSS treatment (week 1, **second column**), and 3 weeks after terminating DSS treatment (week 4, **fourth column**). The EP701Y antibody detects the N terminus of APC, and its specificity has been validated in our previous study.[16] APC expression (brown) was mainly detected in the cell membrane and cytoplasm of mucosal epithelial cells of F344 and KAD rats without DSS administration (**arrows**). The localization of APC changed to vascular endothelial cells in the submucosa of the inflamed distal colon induced by DSS at week 1 (**arrowheads**). The larger views of the **boxed areas** are shown in the **third column**. Scale bar = 20 μm. APC was detected in both mucosal epithelial and vascular endothelial cells at week 4. KAD rats had exactly the same pattern of changes in APC expression as F344 rats. **B:** IHC for CD31 in serial sections of F344 rats at week 1 (**arrowhead**). The image was captured at the same position as that in **A** (above) at week 1. Scale bar = 100 μm.

were observed in KAD rats. Instead, eosinophilic deposits were observed under the lamina propria of KAD rats.

At week 4, the inflammatory changes and mucosal ulcers were resolved for F344 rats, healed by regenerative crypt cells associated with a reduction of the number of inflammatory cells. Severe inflammation was still present in the distal colon of KAD rats, and elongation of the squamous epithelium caused by squamous metaplasia was observed near the border between the rectum and anus. Immune cells, predominantly eosinophilic granulocytes, were continuously observed in the inflamed colon of KAD rats.

Consistent with the histopathologic observations, inflammatory cytokines and mediators, such as *Tnfα*, *Il1β*, *Ptgs2/Cox2*, and *Ptges*, and the anti-inflammatory cytokine *Il10* were expressed in the inflamed distal colon of DSS–treated KAD and F344 rats (Table 1). The cytokines were most highly expressed at week 2 in KAD and F344 rats. At week 4, the expression of those cytokines decreased in the DSS–treated F344 rat colons. In DSS–treated KAD rat colon, the expression of those cytokines was significantly higher than in F344 rats at week 4. These findings indicate that colitis in KAD rats was remarkably persistent even 3 weeks after termination of DSS treatment.

To assess cell proliferation in the mucosal epithelia, we measured the BrdU-labeling index for the colon epithelia. At week 1, few crypts were observed because of the disrupted architecture of the mucosa or ulceration. Thus, indices could not be calculated. At week 2, the indices were not different between KAD and F344 rats. At week 4, the index for the KAD rats was approximately half of that at week 2 but was significantly higher than that of the F344 rats (Table 2). These findings indicated greater persistence of cell proliferation in the KAD rats compared with the F344 rats at week 4.

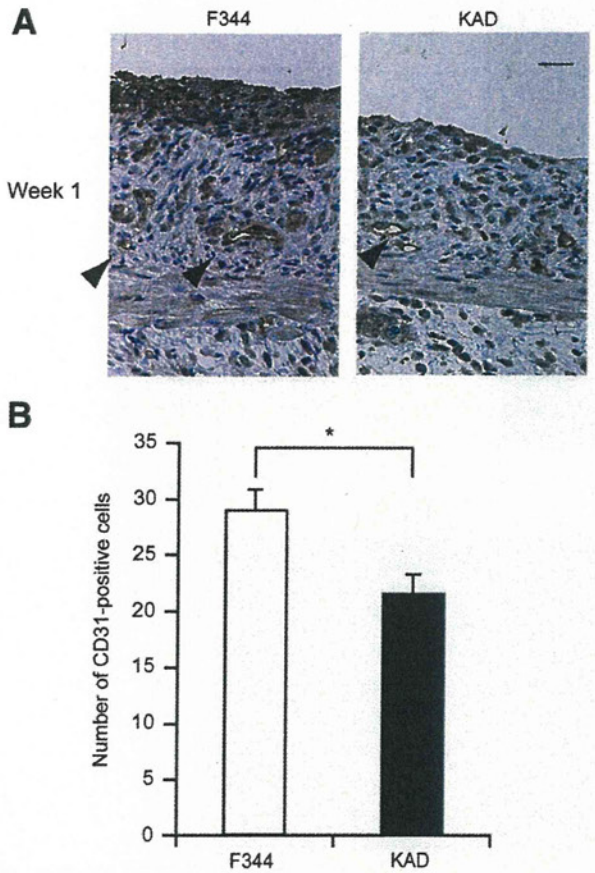

Figure 4 Reduction of angiogenesis associated with an absence of fibrin pseudo-membrane in the DSS-treated colon of KAD rats. **A:** IHC for CD31 of the distal colon of F344 and KAD rats at week 1. CD31-positive cells were clearly present along the ulcerated mucosa of F344 rats, whereas these cells were observed in much smaller numbers in the mucosa of KAD rats (**arrowheads**). Scale bar= 50 μm. **B:** Number of CD31-positive cells per field within the mucosa along the inflamed mucosa. $^*P < 0.001$.

The Absence of Fibrin Clots along the Damaged Mucosal Epithelia of KAD Rat Colon

To determine whether the eosinophilic structures that had been observed in the colon of F344 rats at week 1 were fibrin clots, we performed PTAH staining on the colonic tissue sections. For F344 rats, fibrin clots formed a pseudo-membrane covering the surface of the inflamed colonic mucosa (Figure 2A). In contrast, for KAD rats, formation of the pseudo-membrane consisting of fibrin clots was much less. Instead, fibrin was deposited mostly in microvessels immediately below the lamina propria and formed microthrombi. The area of the fibrin clots that covered the inflamed mucosa was significantly higher for F344 rats than for KAD rats (0.56 ± 0.29 mm^2 versus 0.057 ± 0.039 mm^2; $P < 0.001$) (Figure 2B). The area of fibrin microthrombi was significantly greater for KAD rats than for F344 rats (0.060 ± 0.048 mm^2 versus 0.0047 ± 0.0050 mm^2; $P < 0.04$). These results indicate that the formation of fibrin layers was defective over the damaged mucosa of KAD rats. Thus, the damaged mucosa of KAD rats has low potential to form fibrin layers, which make an important contribution to healing the eroded mucosa.

APC Is Expressed in the VECs in the Inflamed Colon

To find a potential association of the presence of APC with colitis, the expression of APC protein was examined in rat colonic tissue. Sequential change of APC expression was generally common in both F344 and KAD rats. At week 0, APC protein was expressed in the cell membrane and cytoplasm of normal mucosal epithelial cells (Figure 3A). At week 1, immediately after DSS treatment, APC protein was highly expressed in VECs in the inflamed submucosa, although no APC could be detected at the mucosal epithelial cells because of their disruption by severe ulceration. At week 4, the expression of APC had recovered in regenerative mucosal epithelial cells and VECs. We confirmed that APC-positive cells in the inflamed distal colon were VECs by immunostaining of serial sections using the anti-CD31 antibody, a positive marker for VECs (Figure 3B). These findings indicate that the expression of APC protein was induced in VECs of the submucosa when colon inflammation occurred.

Reduced Angiogenesis With Inflamed Colonic Mucosa in KAD Rats

Given that APC protein functions in VECs, we examined microvessel angiogenesis in the damaged mucosa by measuring the number of CD31-positive cells in the damaged colonic mucosa at week 1. For F344 rats, many CD31-positive cells were present along the mucosa, which was often associated with the presence of fibrin-like clots (Figure 4A). For KAD rats, fewer CD31-positive cells were observed. The number of microvessels per field along the inflamed mucosa of KAD rats was significantly lower than that of F344 rats (21.70 ± 1.59 versus 29.10 ± 1.83; $P < 0.001$) (Figure 4B). These results indicate that microvessel angiogenesis for healing was reduced in the damaged mucosa of KAD rats compared with F344 rats.

Truncated APC of KAD Rats Does Not Affect Wnt Signaling

To clarify whether a loss of the C terminus of APC could affect the regulation of Wnt signaling, we cultured REFs from E12.5 embryos of F344 and KAD rats. We then tested these REFs for their ability to inhibit Tcf-regulated transcription in transfection assays. TOPFLASH luciferase activity in the REFs from F344 and KAD rats was similar to control FOPFLASH activity. Luciferase activity in the REFs of both F344 and KAD rats increased with Wnt3a treatment (Supplemental Figure S1). These results indicate that truncated APC of KAD rats can normally regulate the Tcf-regulated transcription through a Wnt ligand.

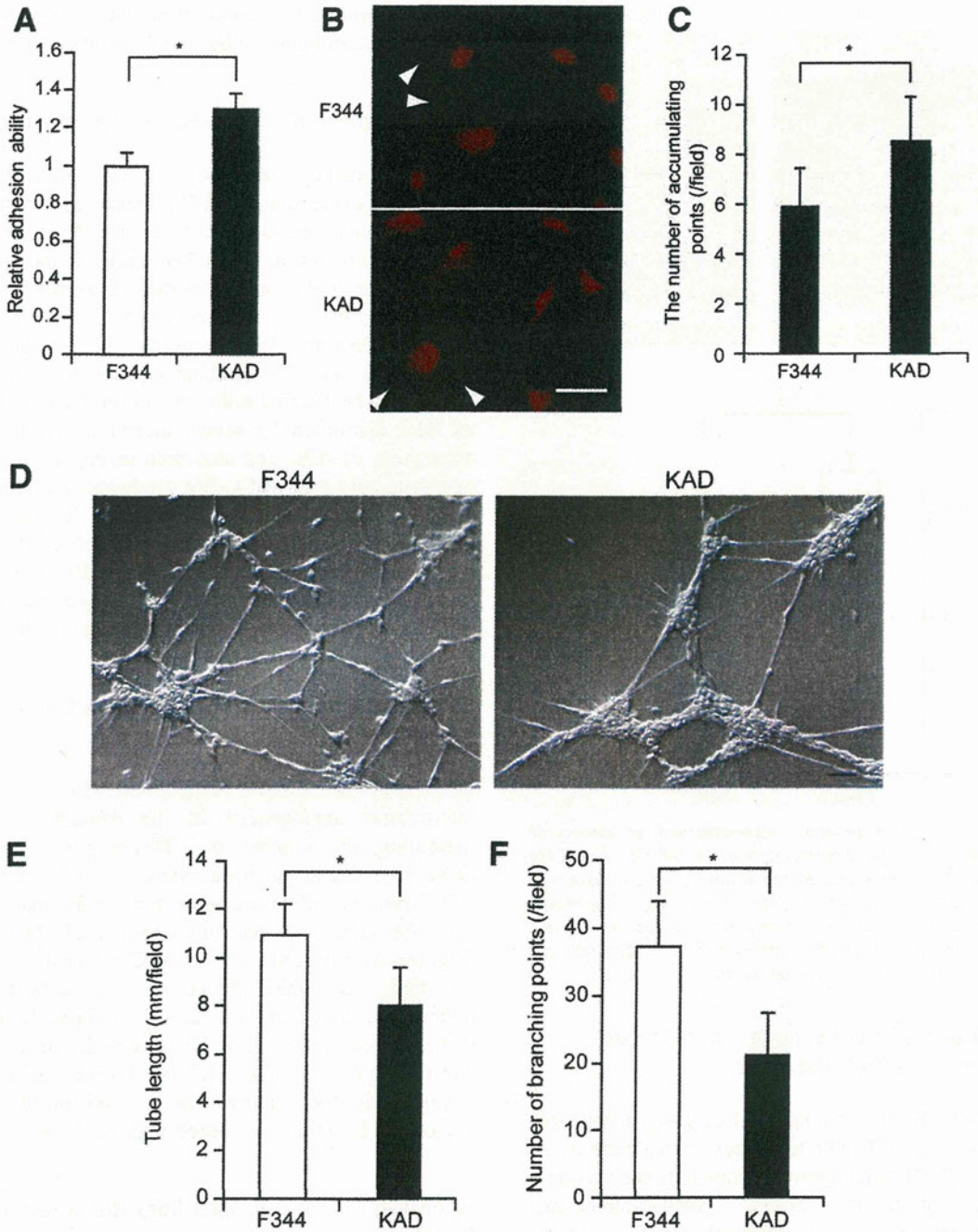

Figure 5 Involvement of APC in endothelial cell tube formation and adhesion. **A:** Wash assay for quantification of adhesion activity of F344 and KAD rat VECs incubated for 30 minutes on collagen-coated wells. Data ($n = 8$) are obtained from two independent experiments. *$P < 0.001$. **B:** Immunofluorescence of paxillin in F344 and KAD rat VECs. Accumulation of paxillin was observed around VECs (**arrowheads**). Scale bar = 50 μm. **C:** The number of paxillin-accumulating points as focal adhesions in five different areas at the cell periphery was counted in 20 cells. *$P < 0.001$. **D:** VECs isolated from F344 and KAD rats were plated onto Matrigel, and the formation of tube networks were photographed 24 hours after culture. Scale bar = 50 μm. **E** and **F:** Quantification of tubular length (**E**) and branching points (**F**) per field at ×100 magnification. Data ($n = 20$) are obtained from two independent experiments. *$P < 0.001$.

VECs of KAD Rats Show High Adhesion Activity and Abnormal Tube Formation

Migration, adhesion, and polarity of VECs play an essential role in angiogenesis, and their efficiency relies on dynamic rearrangement of the cytoskeleton.[25,26] To clarify the involvement of APC in angiogenesis, VECs were isolated from the thoracic aorta of F344 and KAD rats, and their physiologic functions were characterized.

KAD rat VECs had no apparent abnormal morphology when compared with F344 rat VECs and had no difference in the distribution or morphology of either MT or actin

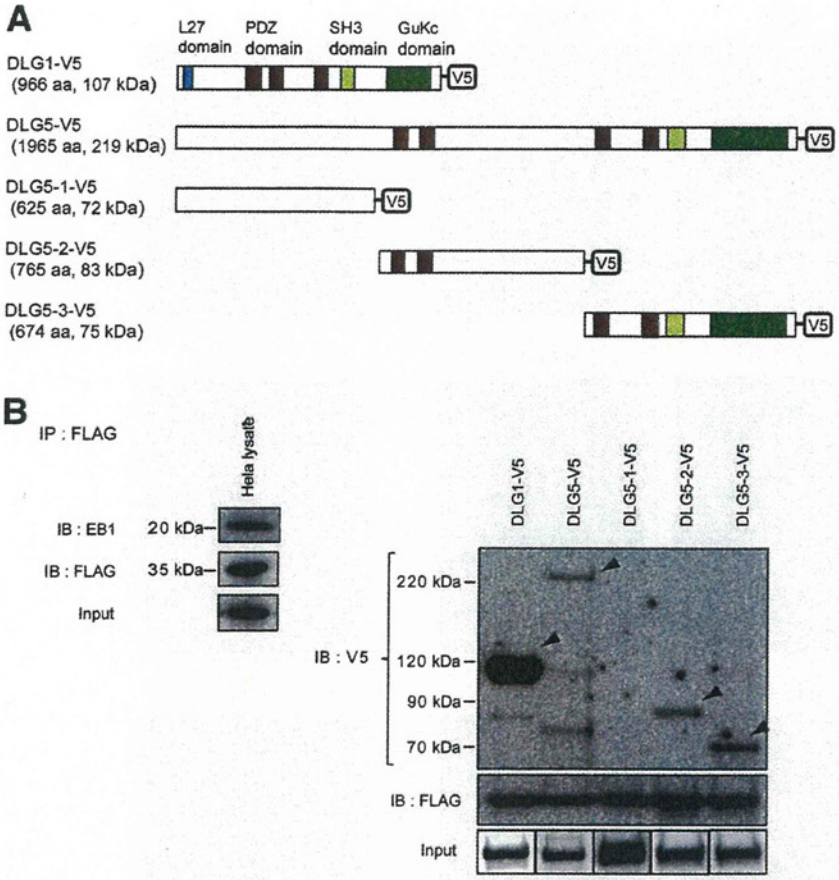

Figure 6 Association of the APC C terminus with EB1, DLG, and DLG5 *in vitro*. **A:** Domain structures and schematic representation of the DLG1 and DLG5 constructs encoding an N-terminal V5 epitope tag: DLG1-V5 (966 amino acids; 107 kDa), DLG5-V5 (1965 amino acids; 219 kDa), DLG5-1-V5 (625 amino acids; 72 kDa), DLG5-2-V5 (765 amino acids; 83 kDa), and DLG5-3-V5 (674 amino acids; 75 kDa). **B:** Binding of the EB1, DLG1, and DLG5 proteins to the FLAG-tagged C terminus of APC (FLAG-APC-C-term; 347 amino acids, 37 kDa) that is absent in the KAD rat. The FLAG-APC-C-term and each construct were co-transfected to Hela cells. The FLAG-APC-C-term was then immunoprecipitated by the FLAG antibody. Immunoprecipitated proteins were subjected to Western blotting to detect proteins that were co-immunoprecipitated with FLAG-APC-C-term. EB1 was detected using the anti-EB1 antibody. DLG1, DLG5, DLG5-1, DLG5-2, and DLG5-3 were detected using the anti-V5 antibody. EB1, DLG1, DLG5, DLG5-2, and DLG5-3 were co-immunoprecipitated with the FLAG-APC-C-term (**arrowheads**).

cytoskeleton. APC protein accumulated at the ends of the MTs at the migrating edges of both F344 and KAD rat VECs (Supplemental Figure S2). The incorporation of BrdU into KAD rat VECs was not different from that seen in F344 rat VECs (F344: 1.00 ± 0.04 versus KAD: 1.01 ± 0.03; $P = 0.92$). A wound healing assay demonstrated that the migration activity of KAD rat VECs stimulated with vascular endothelial growth factor was not different from that of F344 rat VECs (F344: 44.9 ± 6.03 versus KAD: 41.7 ± 7.30; $P = 0.11$).

A wash assay revealed significantly higher adhesion activity in KAD rat VECs than that in F344 rat VECs (Figure 5A). Immunostaining with antipaxillin antibody demonstrated that the number of focal adhesion sites of KAD rat VECs was significantly higher than that of F344 rat VECs (Figure 5, B and C). The capillary-like structure of KAD rat VECs induced on Matrigel revealed apparent differences in morphology compared with those of F344 rat VECs (Figure 5D). The length of tubes of KAD rat VECs was significantly shorter than that of F344 rat VECs (Figure 5E). The number of branches of KAD rat VECs was significantly fewer than that of F344 rat VECs (Figure 5F). These findings indicate that KAD rat VECs had normal physiologic function in morphology, proliferation, and migration but defects in adhesion and tube formation.

EB1 and DLG5 Could Bind to the C Terminus of APC and Are Expressed in the VECs of the Inflamed Colonic Region

To find molecules that interact with the C terminus of APC at the VEC in the inflamed area, we performed an Immunoprecipitation assay and fluorescent IHC. The C terminus of APC, which is absent in KAD rats, can interact with EB1 and DLG1.[12] Recently, DLG5 has been reported to be associated with pathogenesis of IBD.[27] Because DLG5 and DLG1 share the postsynaptic density protein-95/disks large/zonula occludens-1 (PDZ) domains that are known to bind to the C terminus of APC (Figure 6A) and the most characteristic feature of IBD is sustained inflammation of the colon, we examined whether DLG5, similar to EB1 and DLG1, can bind to the C terminus of APC.

Similar to EB1 and DLG1, full-length DLG5 was co-immunoprecipitated with the FLAG-APC-C-term (Figure 6B). Although we could not detect DLG5-1-V5, containing the first third of DLG5, we could detect DLG5-2-V5 and DLG5-3-V5, containing the second and final third of DLG5, respectively (Figure 6B). Both DLG5-2-V5 and DLG5-3-V5 contain PDZ domains, similar to DLG1, but the DLG-1-V5 contained no PDZ domain. Thus, these results indicate that the C terminus of APC could interact with the PDZ domain of DLG5.